Applied Geochemistry 170 (2024) 106048

Contents lists available at ScienceDirect

Applied Geochemistry

journal homepage: www.elsevier.com/locate/apgeochem

Retention of ^{226}Ra in the sandy Opalinus Clay facies from the Mont Terri rock laboratory, Switzerland

Naila Ait-Mouheb [a,*], Yuankai Yang [a], Guido Deissmann [a], Martina Klinkenberg [a], Jenna Poonoosamy [a], Victor Vinograd [a], Luc R. Van Loon [b], Dirk Bosbach [a]

[a] Institute of Energy and Climate Research – Nuclear Waste Management (IEK-6), Forschungszentrum Jülich GmbH, 52428, Jülich, Germany
[b] Laboratory for Waste Management, Paul Scherrer Institut, CH-5232, Villigen PSI, Switzerland

ARTICLE INFO

Editorial handling by: Thomas Gimmi

Keywords:
Sorption
Radium
Opalinus clay
Uptake mechanisms
Modelling

ABSTRACT

The safety assessment of deep geological disposal of nuclear waste requires a sound understanding of radionuclide retention in the repository host rocks. Here, we investigate the retention behaviour of the safety relevant radionuclide ^{226}Ra in the heterogeneous sandy facies of the Opalinus Clay (OPA-SF) at the Mont Terri underground rock laboratory. Various rock samples were selected from a drill core (BAD-1) located in the lower sandy facies, which were representative for its textural and mineralogical heterogeneity. The samples were carefully characterized with respect to mineralogy and chemistry using X-Ray diffraction and electron microscopy. The amounts of quartz, carbonates and clay minerals in the samples ranged between 58 wt.% – 65 wt.%, 13 wt.% – 35 wt.% and 5 wt.% – 25 wt.%, respectively, underpinning the mineralogical heterogeneity. Rare (Ba,Sr)-sulphate precipitates were identified in the clay matrix by electron microscopy. The uptake behaviour of Ra was evaluated using batch sorption experiments. Corresponding to the mineralogical variability of the rock samples, the measured distribution ratios R_d for the ^{226}Ra retention varied between 20 L kg^{-1} and 260 L kg^{-1} after 120 days. The experimental results and thermodynamic modelling approaches suggest that various processes contribute to the uptake of ^{226}Ra on different time scales: fast cation exchange and surface complexation reactions by clay minerals and the (slower) formation of solid solutions during recrystallisation of (Ba,Sr)-sulphates as well as retention by carbonate minerals; the latter mechanism still requiring further investigation.

1. Introduction

Over several years, deep clayey formations are considered as potential host rocks capable of facilitating long term disposal of radioactive wastes. In Switzerland and France these formations lie in Jurassic Opalinus claystones and Callovo-Oxfordian clayrocks. These formations are selected because due to their natural burial depths, the rocks possess very low hydraulic conductivities. Thus, mobility through rock pore water can only occur via molecular diffusion. Due to the high clay mineral content, the diffusing cationic species undergo strong sorption and anionic species undergo anion exclusion. The swelling properties of the clay minerals further facilitate the self-healing of fractures induced during the excavation process. The site "Nördlich Lägern" in the Opalinus Clay in northern Switzerland has recently been proposed as site for a deep geological repository by the Swiss waste management organisation Nagra (2022). Moreover, the Opalinus Clay in southern Germany is also under consideration in the comparative site selection procedure for a repository for heat generating, high-level radioactive waste in Germany (BGE, 2020).

Opalinus Clay has been intensively investigated in the Mont Terri underground rock laboratory (St. Ursanne, canton of Jura, NW-Switzerland, cf. Fig. 1) for more than two decades (Bossart and Thury, 2008; Bossart et al., 2017). The Mont Terri rock laboratory branches off from a security gallery of a motorway tunnel located in the southeast dipping fold limb of the north-west vergent Mont Terri anticline. The thickness of the Opalinus Clay in the rock laboratory is about 130 m with the bedding dipping with approximately 40–45° towards south-east. Opalinus Clay generally consists of dark grey argillaceous to light grey silty-sandy claystones, which can be subdivided into various lithostratigraphic units based on varying quantities of clay minerals (mainly illite, and illite/smectite mixed layers, kaolinite and chlorite), carbonate minerals (predominantly calcite), and quartz (Bossart and Thury 2008; Bossart et al., 2017; Hostettler et al., 2017; Lauper et al., 2018).

The Opalinus Clay can be subdivided into three main lithofacies

* Corresponding author.
E-mail address: n.ait.mouheb@fz-juelich.de (N. Ait-Mouheb).

https://doi.org/10.1016/j.apgeochem.2024.106048
Received 13 October 2023; Received in revised form 30 April 2024; Accepted 21 May 2024
Available online 24 May 2024

types, termed shaly facies, sandy facies, and carbonate-rich sandy facies, differing in mineralogical composition, texture, and homogeneity (e.g., Houben et al., 2014; Hostettler et al., 2017; Lauper et al., 2018, 2021; Kneuker and Furche, 2021). In the Mont Terri rock laboratory, the stratigraphic record comprises, from the lowest to uppermost stratigraphic position (i) the lower shaly facies, (ii) the carbonate-rich sandy facies, (iii) the lower sandy facies, (iv) the upper shaly facies, and (v) the upper sandy facies. The occurrence of the carbonate-rich sandy facies is typical for the Opalinus Clay in north-western Switzerland (Jura region); it does not occur in the proposed siting regions for a geological disposal facility in northern Switzerland (Kneuker et al., 2021). In recent studies, Lauper et al. performed a multi-proxy facies analysis of the Opalinus Clay in Mont Terri (Lauper et al., 2018) and across northern Switzerland (Lauper et al., 2021) to constrain the small-scale heterogeneity of the Opalinus Clay into distinct lithological units, distinguishing five subfacies (SF1 to SF5). According to Lauper et al. (2021), the lower sandy facies of the Opalinus Clay at Mont Terri is largely composed of successions of SF3 (medium grey mudstone of siliceous-argillaceous composition with lenticular to wavy structure and moderate to strong bioturbation) and SF4 (light grey medium to sandy mudstone of calcareous (-siliceous) composition with flaser-bedded to homogeneous structure with strong bioturbation), with rare intercalations of SF2 (dark grey fine to medium mudstone of argillaceous-siliceous composition with lenticular structure and sparse bioturbation).

Compared to the frequently investigated shaly facies of Opalinus Clay in Mont Terri, the sandy Opalinus Clay facies as well as other clay rock formations may exhibit more pronounced compositional and textural heterogeneities (e.g., Lower Cretaceous clayrocks in Northern Germany; Kneuker et al., 2020a). For reliable safety assessment models, an appropriate conceptualization and numerical treatment of these heterogeneities on various scales (from nano-/microscopic scale to m/10 m scale) and upscaling strategies are essential (e.g., Yuan et al., 2022). Radionuclide diffusion in clay rocks is highly dependent on the pore network geometries. In the sandy facies of the Opalinus Clay, this pore network is critically modified due to compositional and textural variability, partly owing to diagenetic reaction products, such as carbonate and sulphide minerals (Philipp et al., 2017), potentially leading to reactive diffusion through heterogeneous physical rock matrix (Kulenkampff et al., 2015).

In long-term safety assessments for radioactive waste disposal, typically a limited number of mobile long-lived fission and activation products such as ^{135}Cs, ^{129}I, ^{99}Tc, ^{79}Se, ^{36}Cl and ^{14}C, as well as decay products from ^{238}U, in particular ^{226}Ra, emerge as the largest contributors to the biosphere dose (e.g., Nagra, 2002; Grambow, 2008; SKB, 2011; IGD-TP, 2020). In this work, we address the effects of the heterogeneity of clay rocks on the retention behaviour of ^{226}Ra as a critical radionuclide to be considered in safety cases for direct disposal of spent nuclear fuels. It may become the dose-dominating radionuclide in the later stages of repository evolution.

Potential mechanisms for ^{226}Ra retention discussed so far include

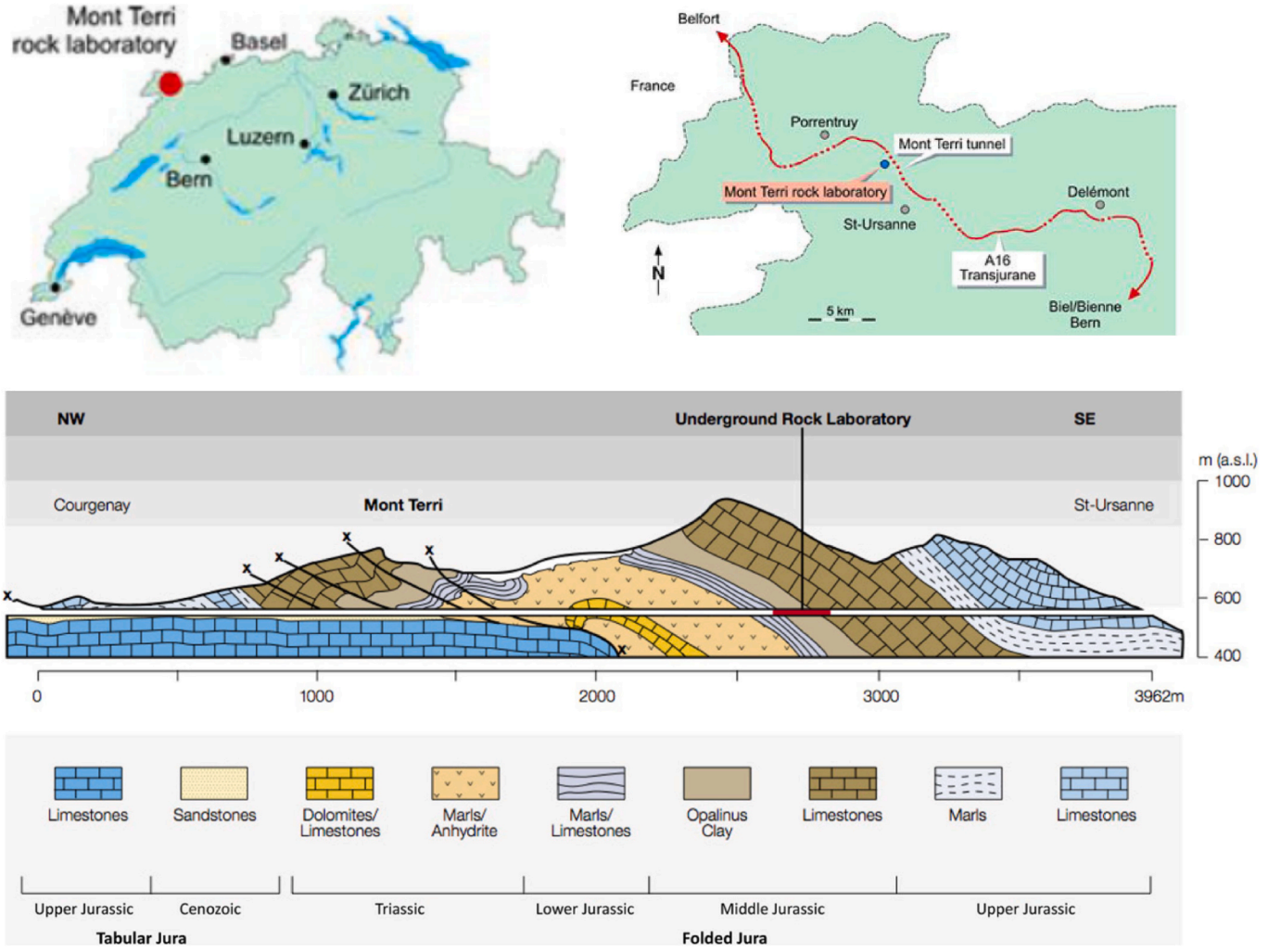

Fig. 1. (a) Location maps of the Mont Terri rock laboratory (from swisstopo, Mont Terri project); (b) Simplified geological profile along the Mont Terri motorway tunnel (from Lauper et al., 2018, with permission).

sorption to bentonite/clay minerals, due to its strong affinity with exchange sites in clay minerals (e.g., Ames et al., 1983; Baston et al., 1993; Tachi et al., 2001; Shao et al., 2009; Chen and Kocar, 2018; Klinkenberg et al., 2021; Marques Fernandes et al., 2023) and incorporation into sulphate minerals such as barite ($BaSO_4$) (e.g., Germann, 1921; Doerner and Hoskins, 1925; Bruno et al., 2007; Klinkenberg et al., 2014; Brandt et al., 2015; Weber et al., 2017). This can occur by recrystallisation of existing (Ba,Sr)SO_4 (Brandt et al., 2020; Vinograd et al., 2013, 2018a, 2018b) in the host rock matrix or also by co-precipitation with barite formed due to reaction of Ba released from the spent nuclear fuel (ca. 5 kg Ba per t uranium) with sulphate-rich groundwaters (Curti et al., 2019). Moreover, based on the chemical similarities of ^{226}Ra and Ba due to their similar ionic radii (r_{Ra}: 164 p.m.; r_{Ba}: 160 p.m. for coordination number XII; Shannon and Prewitt, 1969 and 1970), it has been proposed to also consider the formation of solid solutions with witherite ($BaCO_3$) or strontianite ($SrCO_3$) as solubility limiting process for ^{226}Ra (e.g., Salah et al., 2017). However, data on the retention of ^{226}Ra in clay rocks under scrutiny as potential host rocks for radioactive waste disposal is so far scarce. Therefore, the sorption behaviour of ^{226}Ra in clay rocks is often derived from analogies with Ba or Sr. In particular Ba is deemed as suitable analogue, because of its similarity in ionic radius, electronegativity (0.9 for both ions) and electronic configurations. On the other hand, several studies (e.g., Tesoriero and Pankow, 1996; Yoshida et al., 2008; Missana et al., 2017; Klinkenberg et al., 2021) concluded that the analogy between Sr, Ba and ^{226}Ra with respect to their retention behaviour in clays or clay rocks is not evident, demonstrating the need to quantify the retention behaviour of ^{226}Ra explicitly for potential repository host rocks.

Within the collaborative project *iCross*, a coordinated programme of dedicated laboratory-scale experiments is currently being performed in support of the development of a multi-scale approach to describe and analyse the integrity of nuclear waste repository systems across scales (Bosbach et al., 2021). In this context, the effects of mineralogical, geochemical, and textural heterogeneities of the radionuclide migration in clay rocks in the repository far field were investigated, using the lower sandy facies of the Opalinus Clay from the Mont Terri underground research laboratory, as an example (cf. Chen et al., 2022; Lüth et al., 2024). Therefore, this work is aimed at investigating the retention of the safety-relevant radionuclide ^{226}Ra in the heterogeneous lower sandy facies of the Opalinus Clay. The geochemical and mineralogical characterization of several samples representative of the heterogeneity of the lower sandy facies is performed using X-ray diffraction spectrometry (XRD) and scanning electron microscopy combined with-energy dispersive X-ray spectroscopy (SEM-EDS). Batch sorption experiments were performed to quantify the ^{226}Ra uptake in these materials. For interpretation of the sorption data, geochemical calculations were performed to get insights into the nature and extent of potential sorption processes (e.g. sorption to clay minerals via ion exchange, formation of solid solutions) using a bottom-up approach.

2. Materials and methods

2.1. Drill core samples

The investigated rock samples were taken from the lower part of the BAD-1 drill core, which was drilled within the frame of the AD experiment (i.e. borehole #1 in experiment AD: "Experimental-numerical analysis of discontinuities") with a hole diameter of 131 mm (resulting in a core diameter of 101 mm) parallel to the sedimentary bedding using air as drilling fluid (Galletti and Jaeggi, 2019). The near horizontal borehole BAD-1 with a total length of 15.35 m was drilled from Gallery 4 of the rock laboratory in July 2018 and is located entirely in the lower sandy facies (sandy facies 1) of the Opalinus Clay (Fig. S1 in Supplementary Information). The core samples were conditioned in aluminium foil to avoid desiccation and alteration. The investigated core from the interval 14.35–15.35 m is characterized by a mm-to cm-scale structural and compositional heterogeneity and strong bioturbation (Galletti and Jaeggi, 2019; cf. Fig. 2). A collection of six rock samples representative of the heterogeneity of the material were taken from the central part of the drill core after visual inspection. The outer 2 cm of the core were removed using a diamond saw to avoid issues due to alteration and oxidation processes.

2.2. Characterization of the rock samples

The six selected rock samples (labelled sample 1 to sample 6) were characterised with respect to their physical, mineralogical-geochemical and microstructural properties. The surface area of the crushed and ground material (grain size $\leq$63 μm) was determined by BET measurements with a Quantachrome autosorb analyzer using nitrogen (N_2) as the adsorbate with the multipoint BET method on 1 g of powdered sample. For the determination of the elemental composition of the samples, 50 mg powdered sample were mixed with 0.25 g lithium borate and fused for approximately 30 min at about 1000 °C in a muffle furnace. Subsequently, the fused glass beads were dissolved in 30 ml HCl (5 vol %) and then the aliquots were diluted with 50 ml of Milli Q water (Millipore, 18.2 MΩ cm^{-1} at 25 °C). Two aliquots of each sample solution were analysed by inductively coupled plasma optical emission spectroscopy (ICP−OES) using a Thermo Fisher iCAP 7600 spectrometer. The mineralogical composition of the samples was determined by powder X-ray diffraction (XRD), performed with a Bruker D4 ADVANCE diffractometer using Cu Kα radiation; a step size of 0.02° 2θ and a measuring time of 2 s per time step were applied. For the quantification of the clay minerals of the different materials, a quantitative Rietveld phase analysis was conducted using the GSAS-II software (Toby and Von Dreele, 2013). The microstructure of the materials and the composition/morphology of the minerals were analysed by scanning electron microscopy (SEM) and energy dispersive X-ray spectrometry (EDS) performed using an environmental scanning electron microscope FEI Quanta 200 F equipped with an Apollo X silicon drift detector from EDAX. The accelerating voltage was set to 20 kV and the working distance for the analyses was 10 mm. The preparation of the samples for SEM-EDS measurements was performed by dry cutting of subsamples (1 × 1 cm^2) using a diamond saw at low speed and dry polishing of the samples using SiC paper (down to a grit size of 4000).

2.3. Clay suspensions and equilibrated water

For preparation of the batch experiments, the clay suspensions were conditioned with a so-called synthetic clay pore water. The step-wise method for preparation of this pore water is detailed in Pearson (1998). For five selected samples equilibrated water and Opalinus Clay suspensions were prepared according to the procedure described in Van Loon et al. (2005). Briefly, each sample was ground and sieved in order to obtain crushed rock material with sizes $\leq$63 μm. Subsequently, 10 g of clay powder were placed into dialysis bags (Visking dialysis membrane, Medicell Membranes Ltd, London, UK) together with 80 mL of synthetic Opalinus Clay pore water, following the recipe of Pearson (1998). The pore water was prepared by dissolving the amounts of salts given in Table 1 in Milli-Q water. Two dialysis bags each were placed in a 2 L polyethylene bottle filled with the synthetic pore water. The bottle was shaken gently end-over-end for 4 h after which the solution was replaced by a fresh one. This procedure was repeated four times after which chemical analysis of the major cations indicated that the clay suspensions were in equilibrium with the synthetic pore-water. The last equilibrated water was used to prepare the tracer solutions for the sorption experiments. Each rock suspension inside the dialysis bags was emptied into a quantity of the final synthetic pore water balanced to obtain a S/L ratio of between ~117 and 0.1 g L^{-1}. The exact rock content of the final suspensions was determined by heating weighed aliquots to constant weight at 105 °C and correcting for salt content (Marques Fernandes et al., 2015). The mass of the clay suspension and the solid is

Table 1
Amounts of salts used to prepare 1 L of synthetic Opalinus Clay pore water and its chemical composition (Pearson, 1998).

Salt	Amount of salt (g L^{-1})	Element	Element concentration (mol L^{-1})
NaCl	12.380	Na	$2.40{\cdot}10^{-1}$
KCl	0.120	K	$1.61{\cdot}10^{-3}$
$MgCl_2.6H_2O$	3.457	Mg	$1.69{\cdot}10^{-2}$
$CaCl_2.2H_2O$	3.793	Ca	$2.58{\cdot}10^{-2}$
$SrCl_2.6H_2O$	0.136	Sr	$5.05{\cdot}10^{-4}$
Na_2SO_4	2.00	Cl	$3.00{\cdot}10^{-1}$
$NaHCO_3$	0.040	SO_4	$1.41{\cdot}10^{-2}$
		CO_3/ HCO_3	$4.76{\cdot}10^{-4}$
pH	7.6		
Σ cations	$3.28{\cdot}10^{-1}$ eq L^{-1}		
Σ anions	$3.28{\cdot}10^{-1}$ eq L^{-1}		
Ionic strength	0.39 mol L^{-1}		

given in Table A6 of the Supplementary Material (data publication: Ait Mouheb et al., 2023). The bags are opened and the equilibrated OPA suspensions were stored in polyethylene bottles and used for the batch sorption experiments. The solutions were analysed for cations by ICP–OES (Thermo Fisher iCAP 7600) and for anions by ion chromatography (IC, Thermo Fisher ICS-3000). The composition of the equilibrated waters is given in Table A1 in the Supplementary Material (data publication: Ait Mouheb et al., 2023).

2.4. Sorption experiments

Sorption studies of ^{226}Ra on the crushed and ground materials were carried out in batch-type sorption experiments in a fume hood under atmospheric conditions, since the synthetic pore-water and the rock suspension were in equilibrium with atmospheric CO_2 partial pressure. Dissolved Ra in aqueous systems is not redox sensitive, and its solution speciation is dominated by free Ra^{+2} across a wide range of chemical conditions (e.g., pH, pCO_2 and salinity, cf. Table A2 in Ait Mouheb et al., 2023). The influence of the heterogeneity on the uptake of ^{226}Ra, is demonstrated by five selected samples (samples 1 to sample 5) characterized by strong compositional and structural variation (see Table 4). The samples were investigated in their respective conditioned synthetic pore-water at the corresponding pH (pH of 7.6 and ionic strength of 0.39 mol L^{-1}). The batch sorption experiments were performed using ^{226}Ra concentrations ranging between $2{\cdot}10^{-8}$ M and $2{\cdot}10^{-10}$ M to be below the aqueous solubility limits of Ra-bearing phases under the chemical conditions of the pore water. In Table A2 in the Supplementary Material (Ait Mouheb et al., 2023) the calculated speciation of ^{226}Ra in the Pearson Opalinus Clay water and the saturation indices for Ra-bearing phases are provided (cf. section 2.5). Even at the highest employed ^{226}Ra concentration the solution is strongly undersaturated with respect to pure Ra-phases. Since the composition of the solutions equilibrated with the clay samples is rather similar to the Pearson water (cf. Table A1 in the Supplementary Material, Ait Mouheb et al., 2023), it can be safely assumed that these solutions are also strongly undersaturated regarding the various Ra-phases.

Table 2
Summary of site types, site capacities, and protolysis constants for illite (Marques Fernandes et al., 2023) considered in the model.

Site type	Capacity
High affinity site (HAS)	$5{\cdot}\ 10^{-3}$ eq kg^{-1}
Planar sites (PS)	0.225 eq kg^{-1}
$\equiv S^{w2}OH$	$40{\cdot}10^{-3}$ mol kg^{-1}
Protolysis reactions	**log K**
$\equiv S^{w2}OH + H^+ \Leftrightarrow \equiv S^{w2}OH_2^+$	8.5
$\equiv S^{w2}OH \Leftrightarrow \equiv S^{w2}O^- + H^+$	−10.5

Table 3
Parameters for ^{226}Ra sorption on pure illite (Illite du Puy; Marques Fernandes et al., 2023).

Selectivity coefficient	log K_c (Ra–Na)
Cation exchange reactions	
$2Na\text{-}PS + Ra^{2+} \Leftrightarrow Ra\text{-}PS + 2Na^+$	1.05
$2Na\text{-}HAS + Ra^{2+} \Leftrightarrow Ra\text{-}HAS + 2Na^+$	4.7
SC constants for weak 2 sites	log ^{w2}K
$\equiv S^{w2}SOH + Ra^{2+} \Leftrightarrow \equiv {}^{w2}SORa^+ + H^+$	−3.4

The batch sorption experiments were performed in 40 mL centrifuge tubes using the clay suspensions labelled with ^{226}Ra, covering the required Ra concentration ranges. The suspensions were agitated continuously for up to 120 days by shaking end-over-end. After the specified time, the samples were centrifuged (1 h at 108,000 g max. at 25 °C) and the activities of the tracers in the supernatant solution were determined by ultra-low level liquid scintillation counting (LSC) spectrometer Quantulus (PerkinElmer, USA). After mixing the sample with Ultima Gold LLT cocktail, the cover of the LSC vials were glued gas tight with epoxy resin to avoid the release of Rn. The LSC measurements were carried out after at least 38 days to ascertain secular equilibrium between ^{226}Ra and its short-lived daughter nuclides (i.e., ^{222}Rn to ^{214}Po) (Klinkenberg et al., 2021). The results of the sorption tests are expressed as the distribution ratio R_d [L kg^{-1}] (see Equation (1)) that corresponds to the ratio of the amount of tracer sorbed onto the solid phase (A_{sorbed}) [mol kg^{-1}_{solid}], and the concentration of tracer remaining in solution ($c_{solution}$) [mol $L^{-1}_{solution}$]:

$$R_d = \frac{A_{sorbed}}{c_{solution}} \qquad \text{Equation 1}$$

This equation can be also written as

$$R_d = \frac{A_{ini} - A_t}{A_t}\ \frac{V}{m} \qquad \text{Equation 2}$$

where A_{ini} [Bq] and A_t [Bq] are the initial tracer concentration in solution and the concentration at time t, respectively, V [L] is the volume of the liquid phase and m [kg] is the mass of the solid phase used in the experiment. The sorption kinetics and isotherm experiments were performed with a solid to liquid ratio (S/L ratio) of 117 g L^{-1}. The selected high S/L were used because of the low sorption values anticipated for ^{226}Ra in the Opalinus Clay. A maximum absolute error in the R_d values was calculated by considering the maximum error in each operation step in the sorption experiments and a simple error propagation scheme.

2.5. Thermodynamic modelling

For the sorption models as well as for the calculation of the aqueous speciation of the components in solution and saturation indices of relevant phases the geochemical code PhreeqC Ver. 3.6.2 (Parkhurst and Appelo, 2013) was employed. The ThermoChimie v.11a thermodynamic database (Consortium Andra – Ondraf/Niras – RWM; Giffaut et al., 2014; Grivé et al., 2015), was used for the thermodynamic modelling. The activities of aqueous species were calculated using the specific ion interaction (SIT) approach (cf. Brønsted, 1922; Guggenheim, 1935; Scatchard, 1936).

The sorption modelling approach uses the procedure of the two Site Protolysis Non-Electrostatic Surface Complexation/Cation Exchange (2SPNE SC/CE) described in Bradbury and Baeyens (2011). In this approach, the sorption of ^{226}Ra on Opalinus Clay is envisaged to take place by cation exchange and surface complexation associated with the clay minerals illite and illite/smectite mixed layers, which are considered as the main sorbing phases in these systems. Parameters for Ra sorption by illite are provided by Marques Fernandes et al. (2023). Thus, the modelling approach uses one cation exchange reaction and three different surface complexes on the so-called strong and weak amphoteric

edge sites. The fixed parameters such as site types, site capacities, protolysis constants, and parameters for ^{226}Ra sorption, are summarized in Tables 2 and 3. It is as well considered in the model that in cation exchange processes, ^{226}Ra competes with Na^{+}, Ca^{2+} and Mg^{2+} for permanent-charge sites in clay limited by the cation exchange capacity (CEC). The CEC values were scaled to the respective 2:1 clay mineral content (Bradbury and Baeyens, 2011). As already applied by Hartmann et al. (2008) and Joseph et al. (2013), a cation exchange capacity CEC of 22.5 meq/100 g for illite was used.

The contribution of the ternary $(Ba,Sr,Ra)SO_4$ solid solution to the retention of ^{226}Ra was simulated with the solid solution tool of PHREEQCv3.6.2 (Parkhurst and Appelo, 2013). The keyword "solid solution" allows operating with non-ideal binary solid solutions or ideal solid solutions with any number of components. Therefore, as PHREEQC does not treat non-ideal ternary solutions, an approximate treatment is necessary. As the miscibility in the $(Sr,Ra)SO_4$ binary system is very limited (Vinograd et al., 2018), the ternary $(Ba,Sr,Ra)SO_4$ system can be effectively split into two separate non-ideal solid solution phases, $(Ba,Sr)SO_4$ and $(Ba,Ra)SO_4$, which PHREEQC can handle. In such a model Ra is taken up only by the latter phase, while the amount of Ba that is available to form $(Ba,Ra)SO_4$ is controlled by the amount and the composition of the main, $(Ba,Sr)SO_4$, phase. Due to this approach, a Ra removal from solution by solid solution formation can only be observed in the simulations when both binary solid solutions are formed as thermodynamically stable phases. The condition for this is that the $Ba/(Ba+Sr)$ ratio in the system has to be larger than the mole fraction of Ba in the $(Ba,Sr)SO_4$ phase. If this condition is not fulfilled, the solid sulphate phase is represented by mono-phase $(Ba,Sr)SO_4$, which does not incorporate any Ra. Consequently, to simulate the Ra uptake by solid solution formation, the total $Ba/(Ba+Sr)$ ratio was varied within a sufficiently wide, though realistic, interval (see Fig. A2, Ait Mouheb et al., 2023).

The Margules parameters for $(Ba,Sr)SO_4$ and $(Ba,Ra)SO_4$ were taken from Vinograd et al. (2018). In these simulations certain amounts of $BaSO_4$ and $SrSO_4$ were added to 1 L of equilibrated water (see Table A1, Ait Mouheb et al., 2023). The molar amount of $(Ba,Sr)SO_4$ phase was adjusted to 0.1–0.4 wt.% of 117 g of imaginary solid, while no other solid compounds besides $(Ba,Sr)SO_4$ and $(Ba,Ra)SO_4$ were included into the system definition. The R_d values resulting from the simulations were scaled to 100 g of solid and 1 L of the aqueous phase.

2.6. First-order adsorption kinetic model

The R_d values measured for different samples could be linked to macroscopically distinguishable parameters such as fractions of clay and carbonate components, the pore water composition, and the equilibration time. A pseudo first-order adsorption kinetic model (Wang and Guo, 2020), $R_d = a\left[1-\exp\left(-t/t_s\right)\right]$, was utilized to fit the measured R_d with time. In this adsorption kinetic model, a is the adsorption capacity at the equilibrium and t_s is the characteristic time to describe how fast to reach the equilibrium state of adsorption. Herein, we hypothesize the linear relationships of the a and t_s values with each of the major mineralogical components. Hence, a multiple linear regression was used to quickly fit the R_d values of ^{226}Ra in this system. Under the conditions of synthetic (equilibrated) Opalinus Clay pore water as aqueous medium, a given S/L ratio and temperature, the sorption of ^{226}Ra in the dispersed systems mainly depends on the mineralogical composition of the clay rocks and the equilibration time. The composition of the clay rocks is approximated here by the three major components clay minerals, carbonates, and quartz. According to Table 4, the sum of weight percentage of carbonates W_{Ca}, clay minerals W_{Cl}, quartz W_{Qu} is close to one. For simplification, we assume that the contributions from other rare minerals such as K-feldspar to R_d are ignorable. Therefore, a simple nonlinear fitting relation (equation (3)) is proposed to predict the R_d ($L\,kg^{-1}$) of ^{226}Ra in the sandy Opalinus Clay facies with respect to its simplified normalised mineralogy and the equilibration time t (days):

$$R_d = (a_1 W_{Ca} + a_2 W_{Cl} + a_3 W_{Qu})\left[1-\exp\left(\frac{-t}{a_4 W_{Ca} + a_5 W_{Cl} + a_6 W_{Qu}}\right)\right], \quad \text{Equation 3}$$

with six fitting parameters a_1 to a_6. The fitting parameters a_1 to a_6 do not have any physical meaning, but if the value of W_{Ca}, W_{Qu} and W_{Cl} of a sample are known, we can calculate the a and t_s, which have real physical meaning based on the adsorption kinetics model.

3. Results and discussion

3.1. Characterization of the rock samples

Fig. 2 shows the investigated interval of drill core BAD-1 and an exemplary cross section, illustrating the mm- and cm-scale heterogeneity of the lower sandy facies of the Opalinus Clay. White coarser-grained quartz-rich layers can be clearly observed, alternating with dark grey fine grained clay-rich zones and including light-yellowish coarse-grained carbonate-rich lenses.

The mineralogical composition of the rock samples is given in Table 4 and illustrated in Fig. 3. The geochemical composition of the samples, calculated on oxide basis, is provided in Table 5. The minerals identified are similar in the different selected samples from drill core BAD-1 and comprise calcite, dolomite/ankerite, siderite, quartz, albite/plagioclase, K-feldspar, illite, illite/smectite mixed layers, chlorite, kaolinite and pyrite, representing the typical mineral association of Opalinus Clay at Mont Terri (cf. Houben et al., 2014; Bossart et al., 2017; Lauper et al., 2018). The main phase quantified in the samples is quartz with contents between 58 and 63 wt.%. The carbonate-rich sandy layers represented by samples 1, 2 and 5 contain only between 5 and 12 wt.% clay in contrast to the clay-rich layers (samples 3, 4) having a higher clay content between 21 and 25 wt.%. The carbonate content in the samples varies between 13 and 35 wt.%. According to Lerouge et al. (2015), Waber and Rufer (2017) and Houben et al. (2014) the mineralogical composition of rock samples from the lower sandy facies of the Opalinus Clay at Mont Terri is highly heterogeneous, with 25–56 wt.% clay minerals (illite, chlorite, kaolinite, and illite/smectite mixed layers), 11

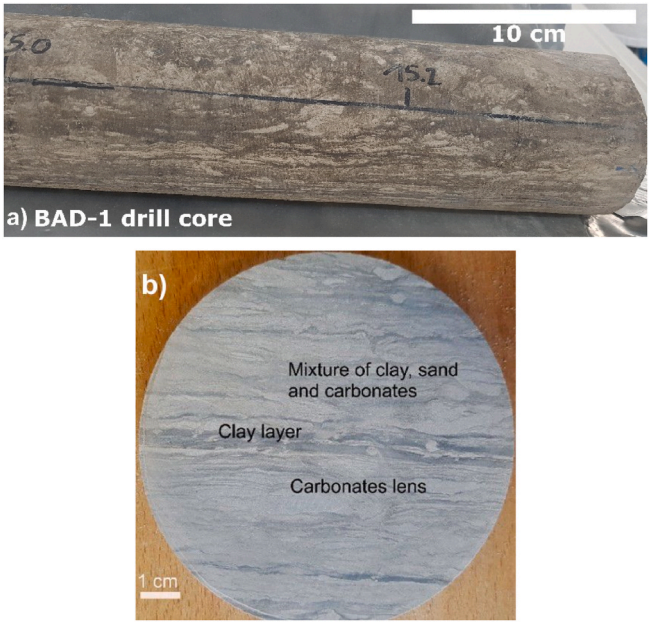

Fig. 2. (a) Investigated interval (15.0–15.35 m) of drill core BAD-1 extracted from the lower sandy facies of Opalinus Clay at the Mont Terri rock laboratory, Switzerland; (b) cross-section of drill core BAD-1.

Table 4
Mineralogical composition (in wt.%) of rock samples from the lower sandy facies of the Opalinus Clay at Mont Terri taken from drill cores BDB-1 (Lerouge et al., 2015; Waber and Rufer, 2017), BWS-H (Houben et al., 2014), and drill core BAD-1 from the present work.

Drillcore	BDB-1	BDB-1	BDB-1	BDB-1	BDB-1	BWS-H	BWS-H	BWS-H	BAD-1	BAD-1	BAD-1	BAD-1	BAD-1	BAD-1
Depth/ description	176.73 m	186.19 m	175.33 m	178.73 m	182.48 m	Clay	Sand	Carbonate	Sample 1	Sample 2	Sample 3	Sample 4	Sample 5	Sample 6
Quartz	32	42	33	45	45	31.4	53.2	11.7	60	61.6	60.9	58.1	65	62.2
K-Feldspar	3	3	5	5	5	3.2[a]	2[a]	0.6[a]	i.d.	3.2	1.8	2.9	2.2	1.8
Plagioclase	3	3	1.7	1.6	1.7				–	–	–	–	–	–
Calcite	8	16	16	19	17	5.1	27.8	69.2	–	–	–	–	–	–
Dolomite/ Ankerite	9	7	6.4	1.1	1.9	0.4	2.4	2	–	–	–	–	–	–
Siderite	3	1	2.4	1.8	2.1	0.9	0	7.3	–	–	–	–	–	–
Kaolinite	9	7	5	7	6	n.s.	n.s.	n.s.	0.3	4.5	6.6	7	5.1	6.4
Illite	14	7	14	7	7	n.s.	n.s.	n.s.	4	5.8	7	9.9	6.1	7.6
Chlorite	1	3	2	4	5	n.s.	n.s.	n.s.	0.7	id.	4.2	5.1	id.	1.1
Illite/ Smectite	14	9	13	7	8	n.s.	n.s.	n.s.	0.1	2.1	3	3.6	1.3	2.2
Anatase	2	2	–	–	–	–	–	–	–	–	–	–	–	–
Apatite	<1	1	–	–	–	–	–	–	–	–	–	–	–	–
Pyrite	2	1	1	0.6	0.6	3	0.2	0.6	<1	<1	<1	<1	<1	<1
Quartz	32	42	33	45	45	31.4	53.2	11.7	60	61.6	60.9	58.1	65	62.2
Carbonate	20	24	24.8	21.9	21	6.4	30.2	78.5	35	22.4	15.2	13.5	20.2	18.7
Clay	38	26	34	25	26	56	14.4	8.4	5.1	12.4	20.8	25.6	12.5	17.3
Source	Lerouge et al. (2015)		Waber and Rufer (2017)			Houben et al. (2014)			Present work					

id. = identified but not quantified.
b n.s.: not specified.
[a] including plagioclase.

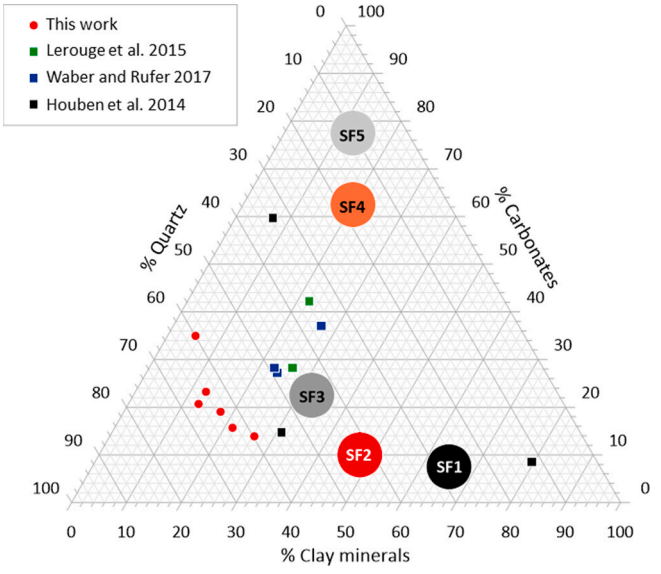

Fig. 3. Ternary diagram illustrating the variation in mineralogical composition of the samples from the lower sandy facies of the Opalinus Clay at Mont Terri (drill core BAD-1) in comparison to data from other drill cores (BDB-1: Lerouge et al., 2015; Waber and Rufer, 2017; BWS-H: Houben et al., 2014) and the average mineralogical composition of Opalinus Clay subfacies SF1 to SF5 according to Lauper et al. (2021). Carbonates include calcite, dolomite and siderite; clay minerals comprise illite, illite/smectite mixed layers, chlorite and kaolinite.

to 53 wt.% quartz and 6 to 78 wt.% carbonates (calcite, dolomite, ankerite, and siderite).

The quantification of the mineralogical composition of drill core BAD-1 indicates that the lower sandy facies in this drill core contains lower amounts of clay minerals and carbonates compared to samples from other drill cores extracted from these facies at Mont Terri (cf. Table 4). This confirms the high compositional heterogeneity of the lower sandy facies of the Mont Terri Opalinus Clay (cf. Kneuker and Furche, 2021). The mineralogical heterogeneity is therefore mainly a question of scale of observation and the representative elementary volumes (REV) of these facies. A difference in the mineralogical composition is to be expected between samples taken on the mm-scale and those selected from the cm- or dm-scale. In this study samples were taken on the cm-scale (sample size approximately 4–5 cm^3) to address explicitly the heterogeneity. However, Steegborn et al. (2024) determined a REV for mineralogy of the lower sandy facies at Mont Terri of 85–100 cm^3, i.e. more than one order of magnitude larger than our samples. In contrast, the REV of the sorption properties with respect to caesium, cobalt and europium was found to be distinctly smaller (8–27 cm^3; Steegborn et al., 2024). In fact, the REVs for different properties of the lower sandy facies affecting radionuclide migration show a distinct spread. From both experimental data and pore-scale modelling predictions, Yuan et al. (2022) demonstrated that the REV for diffusivity (c. 1 cm^3) is larger than the REV for porosity (c. 1 mm^3). The discrepancy between the REV for transport properties such as effective diffusivity and that of porosity were found to become more pronounced in a heterogeneous porous material with lower connectivity and higher tortuosity (Yuan et al., 2022).

According to the sCore classification scheme for organic rich mudrocks (Gamero-Diaz et al., 2013; Glaser et al., 2014), the rock samples taken from core BAD-1 can mainly be classified as mixed siliceous mudstones with one exception (sample 1) classified as carbonate-rich siliceous mudstone (cf. Fig. A1, Ait Mouheb et al., 2023).

The obtained geochemical data largely support the petrographic and mineralogical observations. Generally, Al_2O_3, Fe_2O_3 and K_2O and a high CEC (as a measure of retention capacity) correlate with higher amounts of clay minerals, where the elevated iron content can be attributed to the presence of pyrite. High SiO_2 content is related to sandy, quartz-rich layers, while elevated CaO and MgO correlate with carbonate-rich materials (i.e., presence of calcite and dolomite), though the MgO content

Table 5
Chemical composition (wt.%) of selected rock samples from the lower sandy facies of the Opalinus Clay.

	Sample 1		Sample 2		Sample 3		Sample 4	
	MV	SD	MV	SD	MV	SD	MV	SD
Al_2O_3	8.69	0.21	14.83	0.25	12.58	0.26	22.29	0.57
CaO	11.35	0.13	5.58	0.10	8.73	0.15	3.86	0.10
Fe_2O_3	3.73	0.06	5.72	0.07	5.09	0.07	6.36	0.09
K_2O	1.35	0.04	2.26	0.05	1.84	0.05	2.64	0.05
MgO	0.96	0.02	1.70	0.03	1.58	0.03	2.10	0.02
SiO_2	64.18	6.42	61.83	1.07	59.69	1.07	53.49	1.28
Na_2O	0.42	0.01	0.49	0.01	0.47	0.01	0.47	0.01
SrO	0.12	<0.01	0.03	<0.01	0.05	<0.01	0.02	<0.01
P_2O_5	0.25	<0.01	0.31	0.01	0.30	<0.01	0.20	<0.01
Cr_2O_3	0.01	<0.01	0.02	<0.01	0.01	0.00	0.02	<0.01
SO_3	0.95	0.05	1.00	0.125	1.00	0.05	1.02	0.05
Total	92.01		93.78		91.34		92.48	

MV = Mean Value.
SD = Standard deviation.

may also be bound to the clay-rich matrix in Opalinus Clay (cf. Kneuker et al., 2017; Kneuker and Furche, 2021). Generally, the data agree well with the compositional ranges for the lower sandy facies provided Kneuker and Furche (2021) based on samples from drill core BAD-2, which was located in the vicinity of BAD-1. The variations in geochemical composition are additionally visualized in Fig. 4, using the ternary diagram CaO (as proxy for carbonates), SiO_2 (as proxy for quartz) and Al_2O_3 (as proxy for aluminosilicates such as clay minerals) according to Brumsack (1989), indicating the high compositional variability of the lower sandy facies. Generally, the lower sandy facies (and the carbonate-rich sandy facies) are deemed to represent the more heterogeneous facies endmembers when compared to the well characterized lower shaly facies, which represents the most homogeneous facies in terms of composition (Kneuker and Furche, 2021).

The mineralogical and geochemical heterogeneity of the rocks from BAD-1 in the mm-µm scale is exemplarily illustrated in Fig. 5, depicting SEM images (back scattered electron mode) of a quartz-bearing carbonate lens and a clay rich-layer and corresponding elemental maps of calcium, silicon, sodium, magnesium, and iron obtained by SEM-EDS. In the carbonate lens, irregular shaped aggregates of calcite and quartz are dominating with accessory siderite and interdispersed clay minerals. In the clay rich layer, quartz and minor calcite are embedded within the

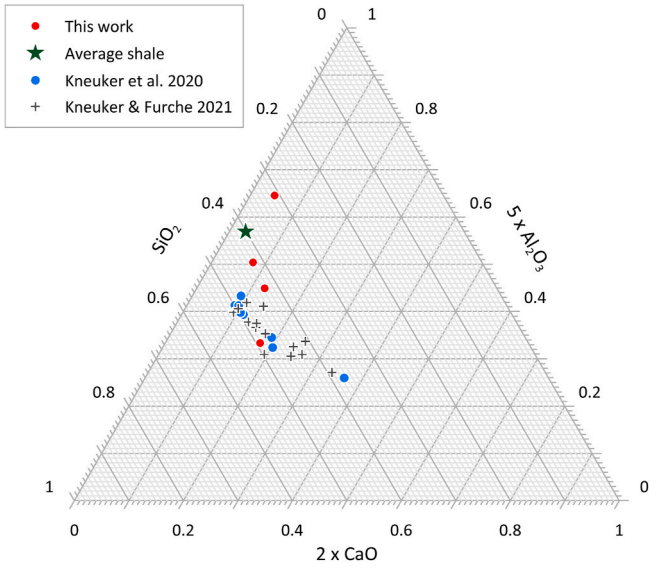

Fig. 4. Ternary diagram $SiO_2 - 5 \times Al_2O_3 - 2 \times CaO$ after Brumsack (1989), showing the variability in the geochemical compositions of the samples from the lower sandy Opalinus Clay facies from the BAD-1 drill core. Composition of the average shale according to Wedepohl (1971).

fine-grained clay matrix, containing also minor amounts of framboidal pyrite. Accessory minerals observed in clay-rich parts of the rock samples comprised (Ba,Sr)-sulphate solid solutions embedded in the clay matrix and framboidal to euhedral pyrite in the clay matrix or in pores (Fig. 6). The chemical composition of the (Ba,Sr)-sulphate determined by SEM-EDS analyses is given in Table A4 (Ait Mouheb et al., 2023), indicating a Sr-rich solid solution.

(Ba,Sr)-sulphates such as celestine and barite, which might be important with respect to the retention of ^{226}Ra, were described to occur in veins, concretions or dispersed in the clay matrix of the Opalinus Clay at Mont Terri (cf. Waber and Schürch, 2000; Gaucher et al., 2003; de Haller et al., 2014; Lerouge et al., 2015; Waber and Rufer, 2017). Lerouge et al. (2015) and Pekala et al. (2019) observed rare (Ba, Sr)-sulphates in the lower sandy facies of the Opalinus Clay at Mont Terri by optical and electron microscopy. The heterogeneously distributed sulphate minerals, partly cementing detrital quartz and feldspar, were described as celestine with Ba contents up to 27 at.% based on EDS spot analyses with evidence of strong chemical zoning on the micrometre scale. Bossart and Thury (2008) assumed a concentration range for both, barite and celestine, in Opalinus Clay at Mont Terri between 0 and 1 wt.% with a best estimate of 0.25 wt.%. Based on the detection limit of their XRD analyses, Waber and Rufer (2017) concluded that the content of sulphate minerals in their samples, if present, was below 0.5 wt.%. Gaucher et al. (2003) determined a celestine content in the shaly Opalinus Clay facies of 0.02–0.06 wt.% based on whole rock geochemical analyses. Geochemical data for the lower sandy facies of the Opalinus Clay at Mont Terri from Kneuker et al. (2020, 2021) show that the Ba and Sr concentration in the rock samples (drill cores BAD-2 and BEP-1) rarely exceed 500 ppm. Using the mean concentration values reported in Kneuker et al. (2020, 2021) and assuming that all Ba and Sr is bound to barite and celestine, respectively (thus neglecting incorporation into rock forming minerals like K-feldspar, micas, or calcite and sorption to clay minerals), provides average concentration levels of the sulphate minerals barite and celestine of about 0.05 and 0.08 wt.%, respectively, in the lower sandy facies of Opalinus Clay at Mont Terri.

3.2. ^{226}Ra retention in the sandy Opalinus Clay facies

3.2.1. Sorption kinetics

The results of the kinetic ^{226}Ra batch sorption experiments are shown in Fig. 7 for the three different initial Ra concentrations; the respective R_d values are listed in Table A5 (Ait Mouheb et al., 2023). An increase of ^{226}Ra uptake over time is observed, indicating a kinetically controlled uptake process. A steady state is not reached even after an experimental duration of 120 days. Generally, ion exchange and surface complexation as uptake mechanisms for cations in clay rocks are known to be rapid and reversible (Singh, 1978). This suggests that potentially other

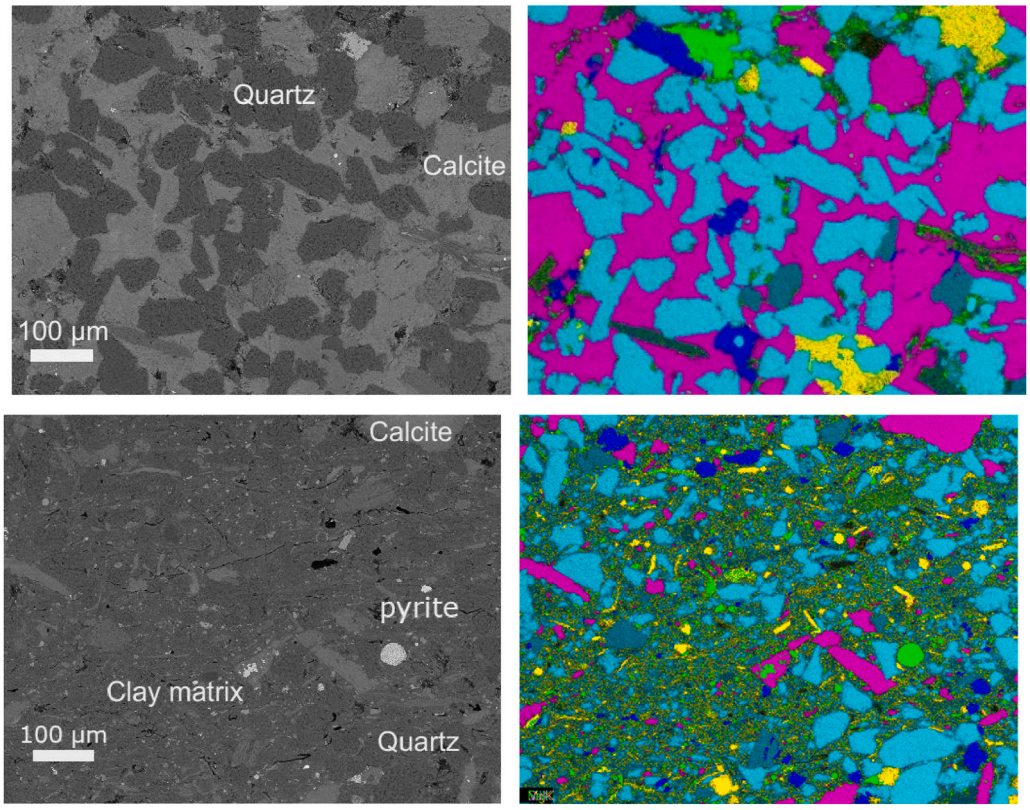

Fig. 5. Left: Backscattered electron SEM images of a quartz-carbonate lens (top, Yuan et al., 2022) and a clay rich layer (bottom) from the lower sandy facies of the Opalinus Clay from drill core BAD-1. Right: False colour SEM-EDS elemental maps overlaid on the SEM images (colour code: pink – calcium, blue – silicon, dark blue – sodium, yellow – magnesium, green – iron).

additional and slower uptake mechanisms for ^{226}Ra such as uptake by recrystallisation of (Ba,Sr)-sulphates, diffusion or incorporation into carbonates through co-precipitation or surface reactions may have to be taken into account in this material (cf. Missana et al., 2017).

A first-order adsorption kinetic model (cf. section 2.6) was employed to describe the kinetic ^{226}Ra sorption experiments. There are three major components (quartz, clay, carbonates) so at least three samples are needed to characterize the effect of mineralogical heterogeneity on the ^{226}Ra retention. Therefore, the experimental data of samples 1, 3, and 4 (cf. Fig. 7) were used as training data. The unknown six parameters in equation (3) were determined by fitting with the training data. After the fitting using MATLAB, the values of the fitting parameters are:

$a_1 = 1872$ L kg^{-1}, $a_2 = 1037$ L kg^{-1}, $a_3 = -748$ L kg^{-1}, $a_4 = 222$ days, $a_5 = 138$ days, and $a_6 = -74$ days.

In Fig. 7 the experimentally derived R_d values are compared with the R_d values calculated by equation (3) as function of time. Next, sample 2 was utilized to test the proposed model. As illustrated in Fig. S2 in the Supplementary Information, the predicted values using the proposed approach without direct fitting agree with the corresponding experimental data of sample 2. In sample 2, using the weight percentage of three major components, t_s is calculated as 21.4 days. Using this equation to calculate t_s will be helpful for future experimental designs.

3.2.2. Distribution ratios

The results of isotherm experiments performed with ^{226}Ra are shown in Fig. 8 for an experimental duration of 30 days and 120 days, respectively. Fig. 8 also shows the corresponding predictions of the PhreeqC calculations assuming ion exchange on illite, which are discussed further below. For all samples, the R_d values for ^{226}Ra are constant in the investigated concentration range. A similar trend in R_d values was observed in a study of ^{226}Ra uptake by Cretaceous clays by Missana et al. (2017). If the materials studied were pure illite, the constant values of R_d could be explained by saturation of the sorption sites. Regarding the uptake of Ra via the formation of (Ba,Sr,Ra)SO_4 solid solution, the constancy of R_d values (Fig. 8), could be traced down to the fixed amount of $BaSO_4$ available in the rock for Ra removal from the aqueous phase. Indeed, considering equation (2) and the approximate proportionality between A_t and the fraction of $BaSO_4$ in the rock (the dilution effect, Bruno et al., 2007), this would explain the constancy of R_d as a function of equilibrium Ra concentration in solution. Regarding carbonate solid solutions, similar trends would have been observed. However, studies by Jones et al. (2011) showed an increase in the distribution ratios, R_d, of ^{226}Ra by carbonate minerals as a function of equilibrium Ra concentration. The results of Jones et al. (2011) seem to suggest that the mechanisms for ^{226}Ra uptake by carbonate minerals could be different from those established for sulphate solid solutions.

The R_d values of the investigated samples from the lower sandy Opalinus Clay facies ranged between 20 L kg^{-1} < R_d < 260 L kg^{-1}, indicating that the mineralogical and geochemical heterogeneity of the sandy Opalinus Clay facies introduces also a heterogeneous retention capacity for ^{226}Ra, as expected – at least on the scale of the investigated samples.

The sorption of ^{226}Ra on illite is envisaged to happen by cation exchange on basal/interlayer surfaces and by surface complexation reactions (Marques Fernandes et al., 2023). The sorption of ^{226}Ra on clays and clay minerals correlates with the CEC, therefore the total amount of clay minerals has an impact on the R_d values (Wersin et al., 2022). Ames et al. (1983) determined the following sequence of ^{226}Ra sorption affinity for different clay minerals at 0.01 M NaCl: clinoptilolite > nontronite > glauconite > montmorillonite > kaolinite; the authors concluded that ^{226}Ra has a strong affinity to the clay minerals with the highest cation exchange capacity (CEC). Tamamura et al. (2014) also observed the increase of ^{226}Ra retention by clay minerals with the increase of CEC, influenced by the concentration of the background

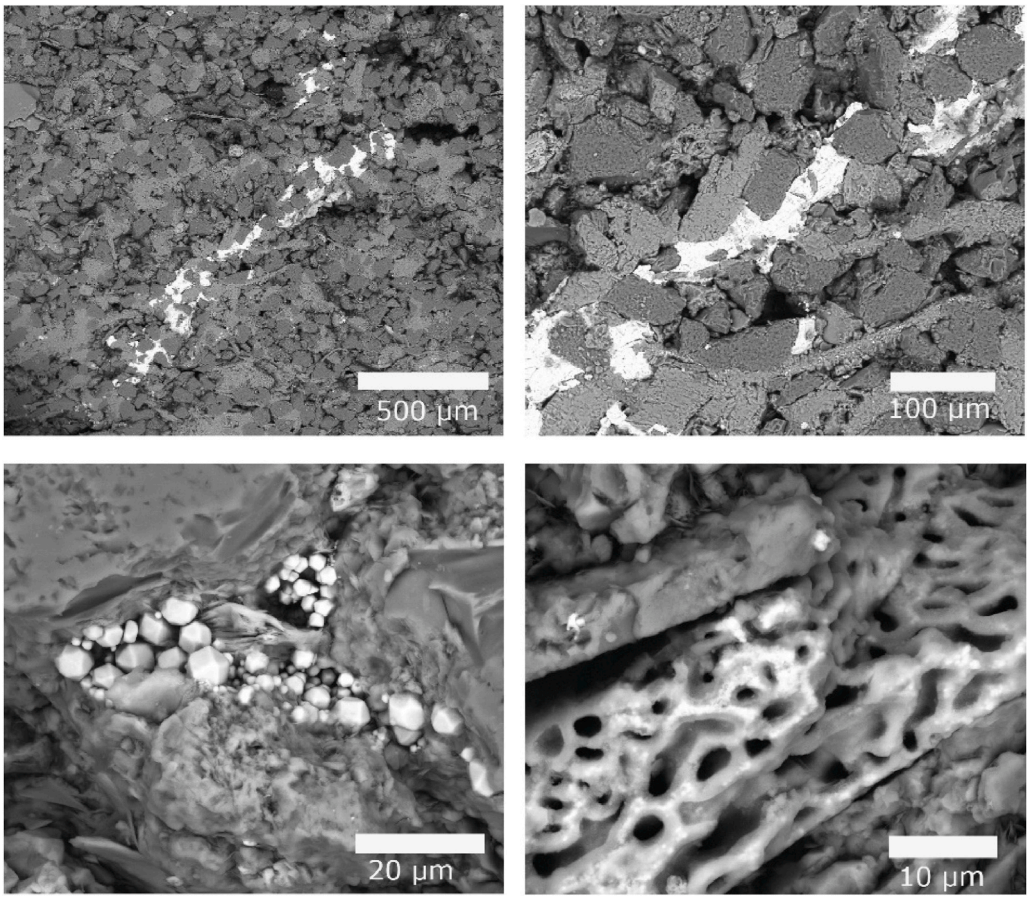

Fig. 6. Accessory minerals and phases observed by SEM (back-scattered electron mode) in clay-rich portions of the lower sandy facies Opalinus Clay from Mont Terri (drill core BAD-1): (Ba, Sr) sulphate (white) embedded in the clay matrix (top), pyrite (bottom left), and fossils (bottom right).

electrolyte.

The predicted ^{226}Ra distribution ratios following the simplified bottom-up approach of Bradbury and Baeyens (2011) and applying the sorption parameters for illite from Marques Fernandes et al. (2023) is shown in comparison to the experimental data in Fig. 8. This modelling approach only assumes ion exchange/surface complexation by clay minerals as uptake mechanism, not considering the formation of Ra-bearing solid solutions with carbonate or sulphate minerals. It can be seen that the experimental data from the batch sorption experiments cannot be reproduced satisfactorily with this approach; the predicted R_d values (3–12 L kg^{-1}) are distinctly lower than the experimental findings. This indicates that additional uptake mechanisms for ^{226}Ra are effective in the sandy Opalinus Clay facies besides sorption to illite and illite/smectite mixed layers.

The investigated rock samples are heterogeneous in terms of mineralogy with clay contents (illite, illite/smectite mixed layers, chlorite and kaolinite) ranging from 5 % to 26 wt.% (cf. section 3.1). In Fig. 9, the R_d values after 45 days are illustrated as function of the mineralogy. Considering the amount of clay minerals presents in each sample and taking into account that Ra has a strong affinity to the material with the highest CEC, one would expect the highest uptake of Ra on sample 4. Nevertheless, the highest R_d value of 260 L kg^{-1} was measured for sample 1, which exhibits the lowest illite content but the highest amounts of carbonates in the investigated materials, suggesting that carbonates (in particular calcite) might play a role with respect to the ^{226}Ra uptake by sandy Opalinus Clay.

The effect of the S/L ratio used in the batch sorption experiments on the R_d value for ^{226}Ra was exemplarily investigated for samples 3 and 5 and is illustrated in Fig. 10 a. The results show that the increase of the S/L ratio from 0.1 g L^{-1} to 117 g L^{-1} leads to a strong decrease of the R_d value, varying over two orders of magnitudes in these samples. These trends in the R_d values are similar to the influence of the S/L ratio on ^{226}Ra sorption on clay materials observed by Missana et al. (2017) and Tamamura et al. (2014). Actually, in systems with higher S/L ratios, an increase of the sorption sites available to the sorbate is anticipated and therefore such experiments should tend to yield “maximum” sorption values, which is not reflected by our data.

In Fig. 10b, the amount of Ra sorbed to the solid phase is depicted as function of the concentration of Ra^{2+} ions in solution (calculated using PHREEQC and the total Ra concentration in solution) at the end of the sorption experiments (i.e., after 45 days). The amount of sorbed ^{226}Ra shows a progressive increase at S/L ratios less than 10 g L^{-1}; a behaviour that is typical for the occurrence of precipitation reactions. However, in a preparatory phase of the sorption experiments, the clay equilibrated solutions spiked with Ra showed constant concentration levels over time, indicating the absence of precipitation of Ra bearing solids. Moreover, PHREEQC calculations of solution speciation and saturation indices of ^{226}Ra phases for Pearson water (cf. Table A2, Ait Mouheb et al., 2023) and solutions equilibrated with the different clay samples revealed that, at the initial ^{226}Ra concentration of $2{\cdot}10^{-8}$ mol L^{-1}, $RaSO_4$ would be distinctly undersaturated in all solutions (SI between −0.85 and −0.90); the solubility limit of ^{226}Ra in the Pearson water would be about $1.4{\cdot}\,10^{-7}$ mol L^{-1} when limited by $RaSO_4$. However, our PHREEQC calculations set with the Pearson water and no solids show that such a system is slightly supersaturated with respect to pure $BaSO_4$. When a small amount of Ra is added, such a system also becomes supersaturated with respect to a $(Ba,Ra)SO_4$ solid solution. The simulated precipitation of $(Ba,Ra)SO_4$ then leads to a slight decrease of the Ra concentration in the aqueous phase. For example, in the experiment with an initial concentration of $1.2{\cdot}10^{-8}$ mol·L^{-1} Ra, the equilibrium

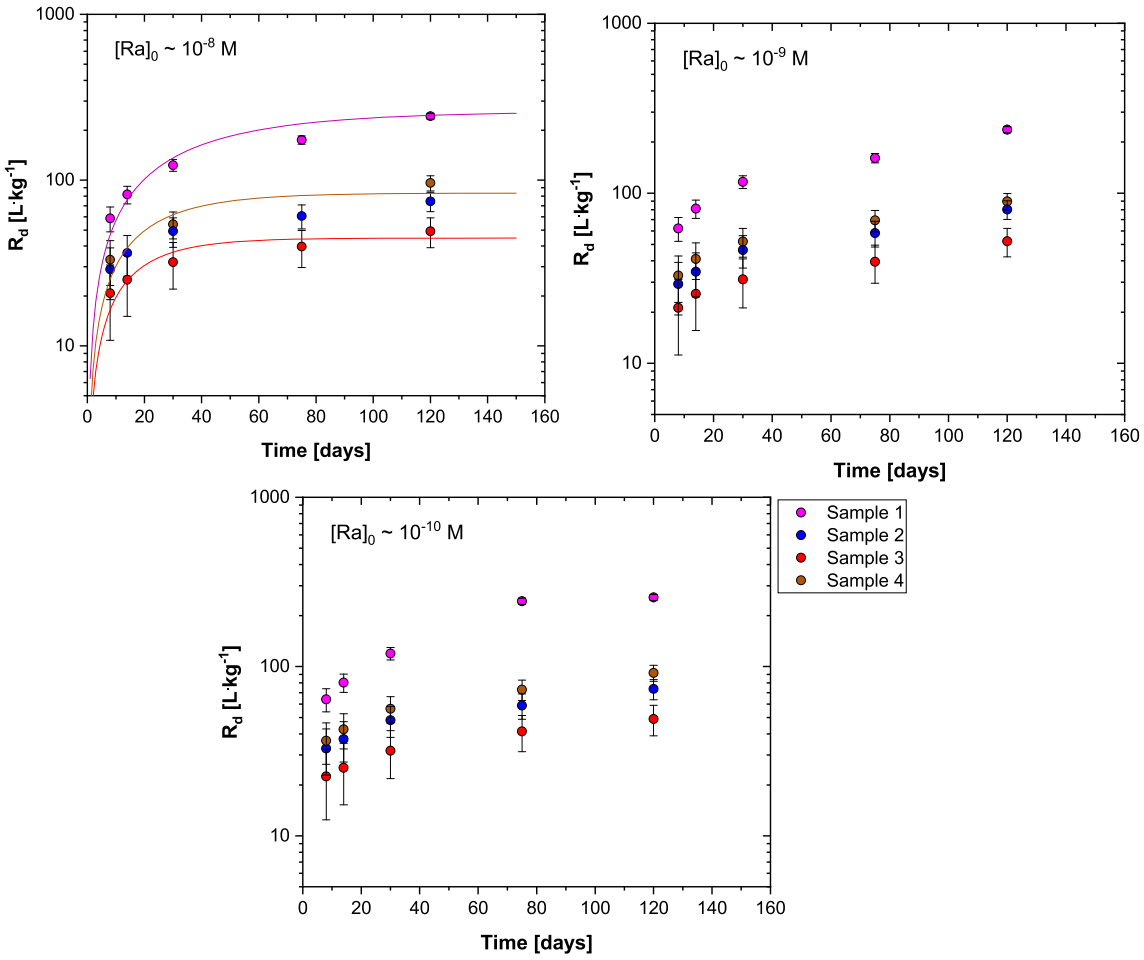

Fig. 7. Sorption of ^{226}Ra on samples from the lower sandy facies of Opalinus Clay (drill core BAD-1) as a function of time (S/L ratio = 117 g L^{-1}; c_0(Ra) ~10^{-8} mol L^{-1} to 10^{-10} mol L^{-1}). The lines correspond to the results of a first-order adsorption kinetic model.

concentration decreases to $8{\cdot}10^{-9}$, i.e. by about 1/3. The latter concentration is very close to the equilibrium Ra concentration observed in the sorption experiment with S/L = 0.1 (Fig. 10c). Based on this observation, we speculate that the drastic increase in calculated R_d values at low S/L ratios could be caused by an effect of precipitation of Ra-bearing $BaSO_4$, which is not considered. We emphasize that such precipitation certainly did not occur in the controlled experiment in which no solids were added. We further speculate that the precipitation of $BaSO_4$ could possibly be triggered by a small amount of solid added to the system in the sorption experiments. The solid particles could act as nucleation centers.

Considering that a certain amount of Ra could be consumed by the precipitation of (Ba,Ra)SO_4, plotting the amount of Ra consumed as a function of S/L provides a misleading interpretation of the sorption capacity of the rock. Plotting the concentration of Ra remaining in solution as a function of the S/L ratio (Fig. 10c) provides a clearer description of the sorption process, suggesting that a certain fixed amount of Ra is consumed via a precipitation reaction that is independent of the amount of solid added. This assumption would explain the very large R_d values at low S/L values (Fig. 10a), calculated using Equation (2), under the assumption that the consumed Ra is equal to the sorbed Ra. A similar effect could be responsible for the very large R_d values reported in other studies assessing the effect of S/L on radionuclide uptake (Missana et al., 2017; Tamamura et al., 2014). It should be noted that if precipitation of (Ba,Ra)SO_4 did indeed occur in the present experiments, the R_d values should be recalculated at all S/L ratios so that the initial concentration of Ra in Eq. (2) decreases consistently with the amount of Ra that has gone into the precipitate. For the experiments with the largest S/L, the R_d values would then decrease by about half. Such a recalculation is not performed here because the proposed precipitation of (Ba,Ra)SO_4 is still considered a hypothesis that requires further investigation.

To our knowledge, no experimentally derived data for the sorption of ^{226}Ra on the sandy Opalinus Clay facies exist so far. Brandt et al. (2019) reported a R_d value of 36.6 L kg^{-1} for the shaly Opalinus Clay facies from Mont Terri. This value, determined at similar experimental conditions (e.g., S/L ratio of 117 g L^{-1}, initial ^{226}Ra concentrations of $1.44{\cdot}10^{-8}$ mol L^{-1} and after 7 days) as in our study, indicates that the geochemical-mineralogical conditions in the sandy Opalinus Clay facies may lead to a higher ^{226}Ra retention capacity than in the more clay-rich shaly facies. In general, data on ^{226}Ra retention by clayrocks are sparse to date. Missana et al. (2017) investigated the retention of ^{226}Ra in lower Cretaceous clay rocks in France as a function of pH, different initial ^{226}Ra concentrations, solid/liquid ratios, and ionic strength. The clay materials from the Gault and Plicatules formations were composed mainly of illite (35–65 wt.%) and illite-smectite mixed layers (25–70 wt. %), In most samples the distribution ratios R_d of ^{226}Ra ranged from 170 to 300 L kg^{-1}. A maximum R_d value of ^{226}Ra of 825 L kg^{-1} was observed for a sample containing 60 wt.% illite and illite-smectite mixed layers, showing the influence of the proportion of clay minerals on ^{226}Ra sorption. The slow kinetics of ^{226}Ra uptake were assumed to be potentially due to precipitation of or incorporation into sulphate and/or carbonate minerals (Missana et al., 2017).

Due to the experimental intricacies when handling ^{226}Ra, experimentally derived retention data for this radionuclide in clays and clay rocks are so far scarce. Therefore, the sorption behaviour of ^{226}Ra is

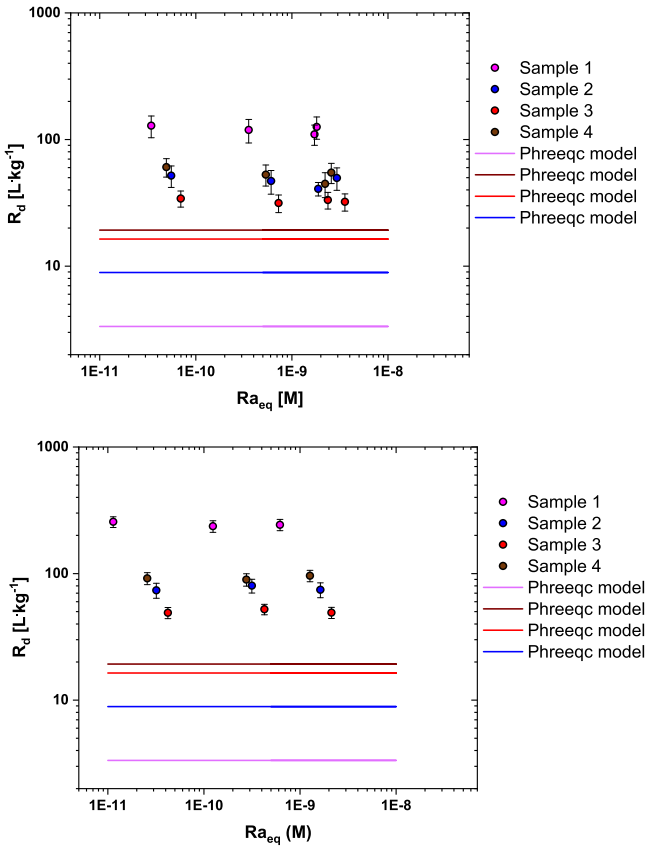

Fig. 8. Sorption isotherms of ^{226}Ra on selected samples from the lower sandy facies of Opalinus Clay from drill core BAD-1 (Mont Terri rock laboratory) after 30 days (top) and 120 days (bottom) equilibration. The coloured lines represent the corresponding predictions by PhreeqC models following a simplified bottom-up approach based on Bradbury and Baeyens (2011), assuming that the retention of ^{226}Ra occurs only by sorption to illite and illite/smectite mixed layers.

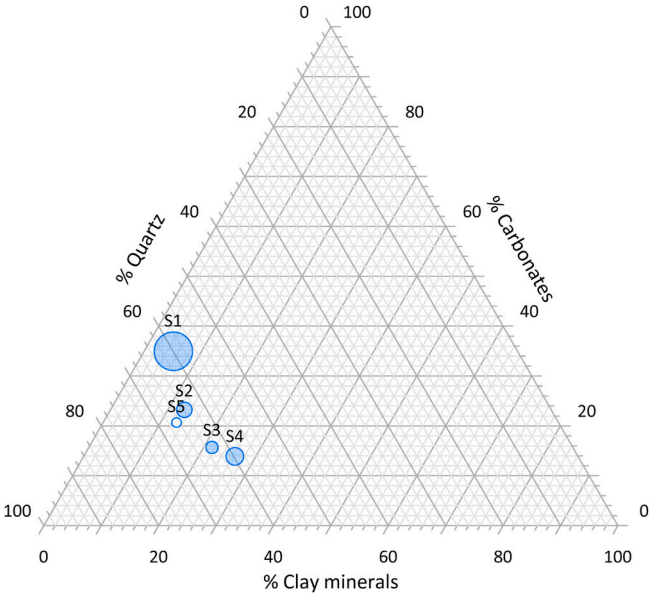

Fig. 9. R_d values for ^{226}Ra for selected samples # 1 to 5 from the lower sandy facies of Opalinus Clay from drill core BAD-1 (Mont Terri rock laboratory) after 120 days equilibration (sample 5: 45 days) in relation to the mineralogy of the rock samples.The respective R_d values are listed in Table 6.

often derived from analogies with Ba or Sr (e.g., Bradbury and Baeyens, 2003a,b; Baeyens et al., 2014; Missana et al., 2017). In particular Ba qualifies as chemical analogue, because of its similarity in ionic radius, electronegativity (0.9 for both ions) and electronic configuration. However, Missana et al. (2017) noted that the selectivity for sorption of ^{226}Ra in the investigated Cretaceous clays was higher than that of Ba by half an order of magnitude; the R_d values of Ba were mainly in the range of 30–90 L kg^{-1}). Moreover, Klinkenberg et al. (2021) found that the selectivity coefficients (K_c) for the cation exchange of Ba and ^{226}Ra with respect to Na on montmorillonite were very similar only at low ionic strength (<0.1 M), whereas at higher ionic strength (0.3 M, i.e. at ionic strengths typically for Opalinus Clay pore water), ^{226}Ra appeared to be more selective. Lauber et al. (2000) investigated the sorption of Sr on the shaly Opalinius Clay facies from Mont Terri at near neutral pH and at a S/L ratio of 241 g L^{-1} with equilibration times of up to six weeks. The authors found distribution ratios of Sr ranging between 1.24 L kg^{-1} and 1.68 L kg^{-1} and suggested that, in addition to cation exchange as an uptake mechanism, Sr had isotopically exchanged with celestine. Moreover, Van Loon et al. (2005) determined slightly lower R_d values for Sr on Opalinus Clay samples from Mont Terri (R_d between 0.64 and 1.3 L kg^{-1}) using batch sorption experiments, through-diffusion and out-diffusion experiments. The R_d values obtained in this work for ^{226}Ra sorption on Opalinus Clay are thus distinctly higher than those obtained with Sr, indicating that Sr is no suitable analogue to derive Ra sorption properties of clays and clay rocks. In the course of the evaluation of electromigration experiments on radionuclide transport in Boom Clay, Maes et al. (2001) also pointed out that the migration parameters of the assumed chemical analogue Sr are not applicable to Ra. Missana et al. (2017) explained these discrepancies in the sorption behaviour of Ra and Sr by the large difference in ionic radii between Ra and Sr (143 p.m. and 112 p.m., respectively, for 6-fold coordination; Shannon and Prewitt, 1969). With the larger ionic radius of Ra, hydration is lower and higher sorption is expected compared to Sr.

3.2.3. *Modelling uptake of Ra by solid-solutions*

As mentioned previously, several studies (e.g., Bruno et al., 2007; Klinkenberg et al., 2014; Brandt et al., 2015; Weber et al., 2017) showed that solid-aqueous equilibria involving barite-type solid solutions can strongly affect the solubility and migration behaviour of ^{226}Ra in the repository environment. Since (Ba,Sr)-sulphates have been observed in the sandy Opalinus Clay facies (cf. Fig. 8 as well as Lerouge et al., 2015; Pekala et al., 2019), their contribution to the uptake of ^{226}Ra was simulated by considering the formation of (Ba,Sr,Ra)SO_4 solid solutions. The simulations aimed to reproduce the formation of celestine containing 65–85 mol% $SrSO_4$. Since the amount of celestine in the investigated samples could not be quantified reliably, a sensitivity analysis was carried out assuming that the quantity of this phase in the sandy Opalinus Clay varies between 0.1 and 0.4 wt.% (cf. Bossart and Thury, 2008). Setting the amount of celestine above 0.4 wt.% would be unrealistic, as this phase would then be observable by XRD. Simulations of Ra-uptake via solid solution formation performed with an ideal ternary solid solution model predicted unrealistically large R_d values ranging between 900 and 1300 L kg^{-1}. The simulations with two non-ideal solid solutions ((Ba,Sr)SO_4 and (Ba,Ra)SO_4; cf. Section 2.5) resulted in more reasonable distribution constants. The results are shown in Fig. S3 in the Supplementary Information and in Fig. A2 in Ait Mouheb et al. (2023). The simulations show that for celestine contents below 0.2 wt.%, the celestine composition becomes too enriched in $BaSO_4$, which is inconsistent with observations. The shift towards Ba-rich compositions occurs due to the high solubility of the $SrSO_4$ component in the aqueous phase. If the amount of celestite phase is set too low, the $SrSO_4$ component dissolves while the mineral is enriched in the remaining $BaSO_4$. Thus, the simulated celestine compositions become similar to the observed compositions in Opalinus clay rocks only when the amount of celestine phase is set between 0.2 and 0.4 wt.%. On the other hand, when the $SrSO_4$ fraction in celestine becomes larger than 70–80 mol%, little

Table 6
Experimental data of 226Ra sorption kinetics on sandy Opalinus Clay at pH 7.6 and I = 0.39 mol·L^{-1} (cf. Fig. 9) with the corresponding mineralogy.

Sample	Duration	log c_0(Ra)	log c_{eql} (Ra)	R_d	log c_0(Ra)	log c_{eql} (Ra)	R_d	log c_0(Ra)	log c_{eql} (Ra)	R_d	Quartz	Carbonate	Clay
	[days]	[mol L^{-1}]	[mol L^{-1}]	[L kg^{-1}]	[mol L^{-1}]	[mol L^{-1}]	[L kg^{-1}]	[mol L^{-1}]	[mol L^{-1}]	[L kg^{-1}]	wt.%		
Sample #1	8	−7.91	−8.74	58.77	−8.59	−9.45	62.1	−9.6	−10.46	63.99	60	35	5.1
	14	−7.86	−8.82	81.92	−8.55	−9.51	81.21	−9.57	−10.52	80.42			
	30	−7.84	−8.96	123.13	−8.54	−9.65	116.69	−9.56	−10.67	119.41			
	75	−7.82	−9.09	174.71	−8.53	−9.76	161.07	−9.54	−10.94	243			
	120	−7.81	−9.21	243.13	−8.51	−9.91	236.64	−9.52	−10.94	256.19			
Sample #2	8	−7.91	−8.53	29.01	−8.59	−9.22	29.25	−9.59	−10.25	32.83	61.6	22.4	12.4
	14	−7.87	−8.56	36.34	−8.55	−9.23	34.57	−9.58	−10.28	37.28			
	30	−7.86	−8.66	49.24	−8.54	−9.32	46.33	−9.57	−10.36	48.22			
	75	−7.84	−8.73	60.73	−8.53	−9.39	58.35	−9.55	−10.42	58.85			
	120	−7.83	−8.79	74.46	−8.51	−9.5	80.21	−9.54	−10.49	73.75			
Sample #3	8	−7.91	−8.45	20.79	−8.59	−9.14	21.18	−9.59	−10.16	22.42	60.9	15.2	20.8
	14	−7.87	−8.47	25.07	−8.55	−9.16	25.6	−9.58	−10.18	25.26			
	30	−7.87	−8.55	31.99	−8.54	−9.21	31.15	−9.57	−10.25	31.81			
	75	−7.85	−8.61	39.72	−8.53	−9.28	39.58	−9.56	−10.33	41.42			
	120	−7.84	−8.67	49.16	−8.51	−9.37	52.23	−9.54	−10.37	49.01			
Sample #4	8	−7.91	−8.59	33.11	−8.6	−9.27	32.81	−9.59	−10.31	36.46	58.1	13.5	25.6
	14	−7.86	−8.62	42.3	−8.55	−9.3	41.12	−9.57	−10.34	42.57			
	30	−7.85	−8.7	54.2	−8.54	−9.38	52.07	−9.56	−10.43	56.34			
	75	−7.83	−8.8	72.42	−8.53	−9.47	69.31	−9.55	−10.51	73.07			
	120	−7.82	−8.9	96.18	−8.51	−9.56	89.61	−9.53	−10.59	91.7			

$BaSO_4$ remains to form the (Ba,Ra)SO_4 phase. Consequently, all Ra remains in the aqueous phase and the R_d value drops to zero. Thus, positive R_d values can only be simulated if the fraction of $BaSO_4$ in celestine is set slightly higher than 15-25 mol%, i.e. slightly higher than the average concentration of $BaSO_4$ reported in celestine from the Opalinus Clay. Fig. S3 shows that under these constraints, the R_d values attributable to ^{226}Ra uptake by celestine solid solution formation would vary in the range of 60–150 L kg^{-1}. This range is in qualitative agreement with the R_d values measured for samples 2–5. However, as discussed above, the average amount of celestine in the lower sandy Opalinus Clay facies at Mont Terri is believed to be less than 0.1 wt.% (see Section 3.1). Thus, until the amount and composition of celestine in the samples are determined with greater accuracy, the efficiency of the Ra uptake mechanism by celestine solid solution would remain questionable.

3.2.4. *Interaction of Ra with carbonate minerals*

The interaction of Ra with carbonate minerals in natural and technical settings has been investigated in several studies (Lange et al., 2018; Jones et al., 2011; Rihs et al., 2000; Yoshida et al., 2008) describing an uptake of Ra by carbonate minerals due to sorption and/or coprecipitation, depending on the nature of the carbonate mineral. Although the ionic radius of Ra^{2+} is too large to be accommodated by the structure of calcite or dolomite (e.g., Curti, 1999; Shao et al., 2009), and although solubilities of carbonate phases are typically larger than solubilities of sulphate phases, it is possible that a yet unidentified Ra-bearing carbonate phase may be formed in systems also saturated with respect to celestine and barite. For example, double carbonates, such as $BaCa(CO_3)_2$, might serve as a possible host for Ra, providing Wyckoff positions with a high coordination number. It has been shown recently that a disordered form of $BaCa(CO_3)_2$ can be formed in a variety of physico-chemical conditions (Spahr et al., 2023; Saito et al., 2020; Whittaker et al., 2021). It has also been demonstrated that large amounts of Ba (and thus presumably also ^{226}Ra) can be entrapped into a disordered calcite-like phase at non-equilibrium conditions when formed via amorphous precursors (ACBC) or during dissolution/recrystallisation of vaterite (Saito et al., 2020; Poonoosamy et al., 2023). Moreover, compared to the uptake of Ra in (Ba,Sr)-sulphate solid solutions, it has to be considered that the amount of carbonates in the sandy Opalinus Clay is significantly larger than the estimated amount of sulphate minerals (cf. section 3.1); thus even a low specific Ra-incorporation into a carbonate mineral could be sufficient to explain the experimentally observed R_d values for ^{226}Ra.

The visual inspection of the drill core and its subsamples, as well as the mineralogical-geochemical and microstructural investigations of the selected rock samples clearly showed the heterogeneity of the lower sandy facies of the Opalinus Clay on various scales. Moreover, the sorption experiments indicate that this heterogeneity extends to the retention behaviour of some safety relevant radionuclides such as ^{226}Ra whose uptake behaviour is strongly affected by mechanisms other than ion exchange/surface complexation by clay minerals, suggesting that the radionuclide retention behaviour in the more heterogeneous lithofacies types of the Opalinus Clay can vary significantly on rather small scales. Each subfacies type (e.g., as defined by Lauper et al., 2018, 2021) may display distinct differences with respect to radionuclide sorption and migration, including also the spatial variability of the pore network and potential heterogeneities with respect to the effective diffusivities (cf. Chen et al., 2022).

In general, it might be expected that dissolved Ra can be retained in sulphate solid solutions, due to the concentration of dissolved SO_4^{2-} present in the investigated clay system. Moreover, the pore water of the Opalinus Clay at Mont Terri is saturated with respect to celestine and barite (Wersin et al., 2022) and (Ba,Sr)-sulphates have been observed in the lower sandy facies (NB: The Pearson water used in the experiments is also saturated with respect to celestine). However, the estimated amounts of (Ba,Sr)-sulphates present in the Opalinus Clay are insufficiently low to explain the observed R_d values of up to about 260 L kg^{-1}. Therefore, taking into account the trend of R_d values with respect to mineralogy (cf. Fig. 9) and the saturation of the Opalinus Clay pore water with calcite (cf. Wersin et al., 2022) it is suggested here that carbonate minerals could also play a role regarding the Ra uptake in the rock samples from the lower sandy Opalinus Clay facies.

4. Conclusions

A good understanding of radionuclide retention capacities and mechanisms in potential repository host rocks such as Opalinus Clay is important for performance assessments of deep geological repositories for spent nuclear fuel and high-level radioactive wastes. To better understand the impact of the natural heterogeneity of clay rocks on radionuclide retention, the uptake and retention of ^{226}Ra by the heterogeneous lower sandy Opalinus Clay facies from the Mont Terri underground rock laboratory was investigated. Various samples

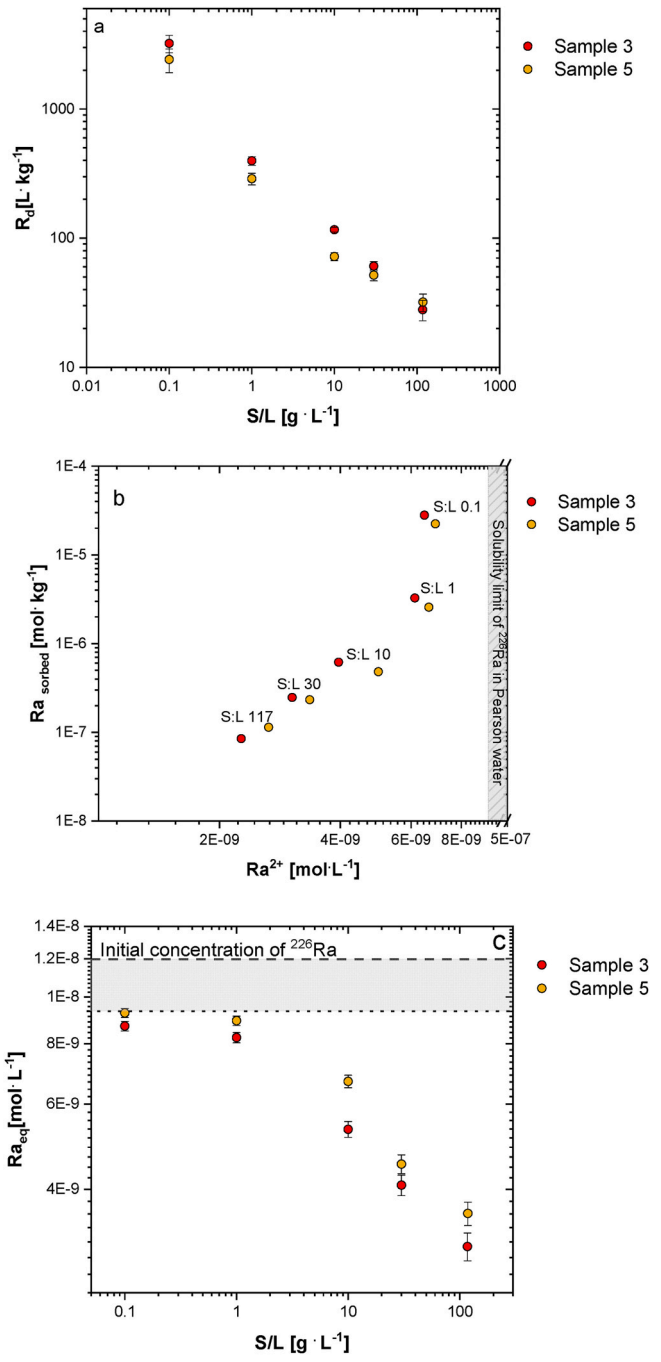

Fig. 10. a) R_d values for sorption of ^{226}Ra on clay rocks from the lower sandy Opalinus Clay facies at Mont Terri as a function of S/L ratio after an experimental duration of 45 days (c_0(Ra) = $1.2{\cdot}10^{-8}$ mol L^{-1}). b) Amount of ^{226}Ra sorbed to selected rock samples from the lower sandy Opalinus Clay facies at Mont Terri for different S/L ratios as function of the concentration of Ra^{2+} ions in the solutions at the end of the batch sorption experiments (i.e., after 45 days). c) The remaining ^{226}Ra concentration in the solution as a function of the S/L ratio. The shaded rectangle corresponds to the change in Ra concentration that has presumably occurred due to precipitation of Ra-bearing $BaSO_4$.

representing the mineralogical and textural heterogeneity of this facies were carefully characterised and their sorption properties with respect to ^{226}Ra were investigated in batch sorption experiments. It could be shown that the mineralogical-geochemical heterogeneity of the sandy Opalinus Clay is also reflected in its sorption behaviour for ^{226}Ra, with distribution ratios, R_d, varying between 50 and 260 L kg^{-1}, thus exceeding those for the shaly Opalinus Clay facies. The experimental results showed that the distribution ratios, R_d, of Ra is constant in the range of investigated Ra concentrations (10^{-8} to 10^{-10} M). The analogies between the sorption behaviour of Ra and Sr (as well as Ba) mentioned in literature is not evident for the sandy Opalinus Clay facies, clearly demonstrating the need to perform experiments with Ra to quantify the retention properties of the repository host rocks adequately. The uptake kinetics and the modelling of the sorption data indicates that beside cation exchange and surface complexation mechanisms of Ra retention other (slow) processes such as uptake by recrystallisation of (Ba,Sr)-sulphates, diffusion or incorporation into carbonates through co-precipitation or surface reactions likely play an important role for the ^{226}Ra uptake in the sandy Opalinus Clay. An approach addressing cation exchange/sorption as the only mechanism of Ra retention underestimated the measured R_d values distinctively. Modelling solid-solution formation of Ra with (Ba,Sr)-sulphates revealed that significantly higher amounts of sulphate minerals in the sandy Opalinus Clay would be required to make this retention mechanism effective and to explain the experimental findings. Thus, based on the mineralogy of the investigated materials it is suggested that carbonate minerals contained in the investigated clay rock could play an important role with respect to the retention of ^{226}Ra. The thermodynamics of incorporation of Ra into carbonate solid solutions and their thermodynamic stability needs to be further investigated. Thus, this study allows for a better understanding of the retention of the safety relevant radionuclide ^{226}Ra in heterogeneous clay host rocks and provides for the first-time quantitative data on its retention behaviour in the sandy Opalinus Clay facies. Moreover, it highlights the requirement of considering and further investigating the formation of Ra-bearing carbonate solid solutions as potential retardation mechanism for ^{226}Ra in carbonate-bearing clays and clay rocks.

CRediT authorship contribution statement

Naila Ait-Mouheb: Conceptualization, Data curation, Formal analysis, Investigation, Methodology, Visualization, Writing – original draft, Writing – review & editing. **Yuankai Yang:** Methodology, Writing – review & editing. **Guido Deissmann:** Conceptualization, Funding acquisition, Project administration, Writing – review & editing. **Martina Klinkenberg:** Methodology, Writing – review & editing. **Jenna Poonoosamy:** Methodology, Writing – review & editing. **Victor Vinograd:** Methodology, Writing – review & editing. **Luc R. Van Loon:** Methodology, Writing – review & editing. **Dirk Bosbach:** Conceptualization, Funding acquisition, Project administration, Resources, Writing – review & editing.

Declaration of competing interest

None.

Data availability

Data will be made available on request.

Acknowledgements

The research leading to these results has received funding from the German Federal Ministry of Education and Research (BMBF, grant agreement 02NUK053A) and from the Initiative and Networking Fund of the Helmholtz Association (HGF grant SO-093) within the *iCross* project. The authors would like to thank KIT-INE for providing the drill core samples. N. A. M. thanks Gabriel Murphy (Forschungszentrum Jülich GmbH) for the precious help in the quantitative Rietveld phase analyses.

Appendix A. Supplementary data

Supplementary data to this article can be found online at https://doi.

org/10.1016/j.apgeochem.2024.106048.

References

Ait Mouheb, N., Yang, Y., Deissmann, G., Klinkenberg, M., Poonoosamy, J., Vinograd, V., Van Loon, L.R., Bosbach, D., 2023. Experimental data for: retention of ^{226}Ra in the sandy Opalinus clay facies from the Mont Terri rock laboratory, Switzerland. https://doi.org/10.26165/JUELICH-DATA/IFD1I9. Jülich DATA, V1.

Ames, L.L., McGarrah, J.E., Walker, B.A., 1983. Sorption of trace constituents from aqueous solutions onto secondary minerals. II. Radium. Clay Clay Miner. 31, 335–342. https://doi.org/10.1346/CCMN.1983.0310502.

Baeyens, B., Thoenen, T., Bradbury, M.H., Marques Fernandes, M., 2014. Sorption data bases for argillaceous rocks and bentonite for the provisional safety analyses for SGT-E2. Nagra Techn. Rep. 12–04, Nagra, Wettingen, Switzerland.

Baston, G.M.N., Berry, J.A., Linklater, C.M., 1993. Factors influencing the sorption of radium onto geological materials. Anal. Proc. 30, 194–195. https://doi.org/10.1039/AP9933000190.

BGE, 2020. Zwischenbericht teilgebiete gemäß § 13 StandAG, Stand 28.09.2020. Bundesgesellschaft für Endlagerung mbH (BGE) Peine.

Bosbach, D., Geckeis, H., Heberling, F., Kolditz, O., Kühn, M., Müller, K., Stumpf, T., the iCROSS team, 2021. An interdisciplinary view of the long-term evolution of repository systems across scales: the iCROSS project. Saf. Nucl. Waste Dispos. 1, 85–87. https://doi.org/10.5194/sand-1-85-2021.

Bossart, P., Thury, M., 2008. Mont Terri rock laboratory project, programme 1996 to 2007 and results. Rep. Swiss Geol. Surv. 3, 1–445.

Bossart, P., Bernier, F., Birkholzer, J., Bruggeman, C., Connolly, P., Dewonck, S., Fukaya, M., Herfort, M., Jensen, M., Matray, J.M., Mayor, J.C., Moeri, A., Oyama, T., Schuster, K., Shigeta, N., Vietor, T., Wieczorek, K., 2017. Mont Terri rock laboratory, 20 years of research: introduction, site characteristics and overview of experiments. Swiss J. Geosci. 110, 3–22. https://doi.org/10.1007/978-3-319-70458-6_1.

Bradbury, M.H., Baeyens, B., 2003a. Far field sorption data bases for performance assessment of a high-level radioactive waste repository in an undisturbed Opalinus Clay host rock. PSI-Rep. 3–8. Paul Scherrer Institut, Villigen, Switzerland.

Bradbury, M.H., Baeyens, B., 2003b. Near field sorption data bases for compacted MX-80 bentonite for performance assessment of a high-level radioactive waste repository in Opalinus Clay host rock. PSI-Rep. 03-07. Paul Scherrer Institut, Villigen, Switzerland.

Bradbury, M.H., Baeyens, B., 2011. Predictive sorption modelling of Ni(II), Co(II), Eu (IIII), Th(IV) and U(VI) on MX-80 bentonite and Opalinus Clay: a "bottom-up" approach. Appl. Clay Sci. 52, 27–33. https://doi.org/10.1016/j.clay.2011.01.022.

Brandt, F., Curti, E., Klinkenberg, M., Rozov, K., Bosbach, D., 2015. Replacement of barite by a (Ba,Ra)SO_4 solid solution at close to equilibrium conditions: a combined experimental and theoretical study. Geochem. Cosmochim. Acta 155, 1–15. https://doi.org/10.1016/j.gca.2015.01.016.

Brandt, F., Van Loon, L., Klinkenberg, M., Poonoosamy, J., Glaus, M., Bosbach, D., 2019. Diffusion of 226Radium through Opalinus clay: combined diffusion and sorption study. Migration 2019, 15–20. September 2019, Kyoto, Japan.

Brandt, F., Klinkenberg, M., Poonoosamy, J., Bosbach, D., 2020. Recrystallization and uptake of ^{226}Ra into Ba-rich (Ba,Sr)SO_4 solid solutions. Minerals 10 (812). https://doi.org/10.3390/min10090812.

Brønsted, J.N., 1922. Studies of solubility: IV. The principle of specific interaction of ions. J. Am. Chem. Soc. 44, 877–898. https://doi.org/10.1021/ja01426a001.

Brumsack, H.J., 1989. Geochemistry of recent TOC-rich sediments from the Gulf of California and the Black Sea. Geol. Rundsch. 78, 851–882. https://doi.org/10.1007/BF01829327.

Bruno, J., Bosbach, D., Kulik, D.A., Navrotsky, A. (Eds.), 2007. Chemical Thermodynamics of Solid Solutions of Interest in Radioactive Waste Management: a State-Of-The-Art Report. Chemical Thermodynamics Series. 10. OECD, Paris, p. 266.

Chen, M.A., Kocar, B.D., 2018. Radium sorption to iron (hydr)oxides, pyrite, and montmorillonite: implications for mobility. Environ. Sci. Technol. 52, 4023–4030. https://doi.org/10.1021/acs.est.7b05443.

Chen, C., Yuan, T., Lu, R., Fischer, C., Kolditz, O., Shao, H., 2022. The influence of sedimentary heterogeneity on the diffusion of radionuclides in the sandy facies of Opalinus Clay at the field scale. Adv. Geosci. 58, 77–85. https://doi.org/10.5194/adgeo-58-77-2022.

Curti, E., 1999. Coprecipitation of radionuclides with calcite: estimation of partition coefficients based on a review of laboratory investigations and geochemical data. Appl. Geochem. 14, 433–445. https://doi.org/10.1016/S0883-2927(98)00065-1.

Curti, E., Xto, J., Borca, C.N., Henzler, K., Huthwelker, T., Prasianakis, N.I., 2019. Modelling Ra-bearing baryte nucleation/precipitation kinetics at the pore scale: application to radioactive waste disposal. Eur. J. Mineral. 31, 247–262. https://doi.org/10.1127/ejm/2019/0031-2818.

de Haller, A., Mazurek, M., Spangenberg, J., Möri, A., 2014. SF (Self-sealing of faults and paleo-fluid flow): Synthesis report (info:eu-repo/semantics/report), de Haller, Antoine; Mazurek, Martin; Spangenberg, Jorge; Möri, Andreas (2014). SF (Self-sealing of faults and paleo-fluid flow): Synthesis report Mont Terri Consortium. Mont Terri Consortium.

Doerner, H.A., Hoskins, W.M., 1925. Co-precipitation of radium and barium sulfates 1. J. Am. Chem. Soc. 47, 662–675. https://doi.org/10.1021/ja01680a010.

Galletti, M., Jaeggi, D., 2019. AD Experiment: drillcore documentation of boreholes BAD-1 and BAD-2. Mont Terri Proj. Techn. Note 2019–06.

Gamero-Diaz, H., Miller, C., Lewis, R., 2013. SCore: a mineralogy based classification scheme for organic mudstones. SPE Annu. Tech. Conf. Exhib 2013 (3), 2465–2481. https://doi.org/10.2118/166284-MS.

Gaucher, E.C., Fernández, A.M., Waber, H.N., 2003. Rock and mineral characterisation of the Opalinus clay formation. In: Pearson, F.J., et al. (Eds.), 2003. Mont Terri Project - Geochemistry of Water in the Opalinus Clay Formation at the Mont Terri Rock Laboratory. Reports of the Federal Office of Water and Geology (FOWG), Geology Series No 5. Federal Office of Topography (Swisstopo). Wabern, Switzerland.

Germann, F.E., 1921. Adsorption of radium by barium sulfates. J. Am. Chem. Soc. 43, 1615–1621. https://doi.org/10.1021/ja01440a025.

Giffaut, E., Grive, M., Blanc, Ph, Vieillard, Ph, Colas, E., Gailhanou, H., Gaboreau, S., Marty, N., Madé, B., Duro, L., 2014. Andra thermodynamic database for performance assessment: ThermoChimie. Appl. Geochem. 49, 225–236. https://doi.org/10.1016/j.apgeochem.2014.05.007.

Glaser, K.S., Miller, C.K., Johnson, G.M., Kleinberg, R.L., Pennington, W.D., 2014. Seeking the sweet spot: reservoir and completion quality in organic shales. Oilfield Rev. 25, 16–29.

Grambow, B., 2008. Mobile fission and activation products in nuclear waste disposal. J. Contam. Hydrol. 102, 180–186. https://doi.org/10.1016/j.jconhyd.2008.10.006.

Grivé, M., Duro, L., Colas, E., Giffaut, E., 2015. Thermodynamic data selection applied to radionuclides and chemotoxic elements: an overview of the ThermoChimie-TDB. Appl. Geochem. 55, 85–94. https://doi.org/10.1016/j.apgeochem.2014.12.017.

Guggenheim, E.A., 1935. The specific thermodynamic properties of aqueous solutions of strong electrolytes. Philos. What Mag. 19, 588–643. https://doi.org/10.1080/14786443508561403.

Hartmann, E., Geckeis, H., Rabung, T., Lützenkirchen, J., Fanghänel, T., 2008. Sorption of radionuclides onto natural clay rocks. Radiochim. Acta 96, 699–707. https://doi.org/10.1524/ract.2008.1556.

Hostettler, B., Reisdorf, A.G., Jaeggi, D., Deplazes, G., Bläsi, H., Morard, A., Feist-Burkhardt, S., Waltschew, A., Dietze, V., Menkveld-Gfell, U., 2017. Litho- and biostratigraphy of the Opalinus Clay and bounding formations in the Mont Terri rock laboratory (Switzerland). Swiss J. Geosci. 110, 23–37. https://doi.org/10.1007/s00015-016-0250-3.

Houben, M.E., Desbois, G., Urai, J.L., 2014. A comparative study of representative 2D microstructures in Shaly and Sandy facies of Opalinus Clay (Mont Terri, Switzerland) inferred form BIB-SEM and MIP methods. Mar. Petrol. Geol. 49, 143–161. https://doi.org/10.1016/j.marpetgeo.2013.10.009.

IGD-TP, 2020. Vision 2040 – strategic research agenda. Implement. Geol. Disp. Radioact. Waste Technol. Platf. (IGD-TP). https://doi.org/10.5281/zenodo.4059860.

Jones, M.J., Butchins, L.J., Charnock, J.M., Pattrick, R.A.D., Small, J.S., Vaughan, D.J., Wincott, P.L., Livens, F.R., 2011. Reactions of radium and barium with the surfaces of carbonate minerals. Appl. Geochem. 26, 1231–1238. https://doi.org/10.1016/j.apgeochem.2011.04.012.

Klinkenberg, M., Brandt, F., Breuer, U., Bosbach, D., 2014. Uptake of Ra during the recrystallization of barite: a microscopic and time of flight-Secondary Ion Mass Spectrometry study. Environ. Sci. Technol. 48, 6620–6627. https://doi.org/10.1021/es405502e.

Joseph, C., Van Loon, L.R., Jakob, A., Steudtner, R., Schmeide, K., Sachs, S., Bernhard, G., 2013. Diffusion of U(VI) in Opalinus Clay: Influence of temperature and humic acid. Geochim. Cosmochim. Acta 109, 74–89. https://doi.org/10.1016/j.gca.2013.01.027.

Klinkenberg, M., Brandt, F., Baeyens, B., Bosbach, D., Marques Fernandes, M., 2021. Adsorption of barium and radium on montmorillonite: a comparative experimental and modelling study. Appl. Geochem. 135 (105117) https://doi.org/10.1016/j.apgeochem.2021.105117.

Kneuker, T., Furche, M., 2021. Capturing the structural and compositional variability of Opalinus Clay: constraints from multidisciplinary investigations of Mont Terri drill cores (Switzerland). Environ. Earth Sci. 80 (421) https://doi.org/10.1007/s12665-021-09708-1.

Kneuker, T., Hammer, J., Shao, H., Schuster, K., Furche, M., Zulauf, G., 2017. Microstructure and composition of brittle faults in claystones of the Mont Terri rock laboratory (Switzerland): new data from petrographic studies, geophysical borehole logging and permeability tests. Eng. Geol. 231, 139–156. https://doi.org/10.1016/j.enggeo.2017.10.016.

Kneuker, T., Blumenberg, M., Strauss, H., Dohrmann, R., Hammer, J., Zulauf, G., 2020a. Structure, kinematics and composition of fluid-controlled brittle faults and veins in Lower Cretaceous claystones (Lower Saxony Basin, Northern Germany): constraints from petrographic studies, microfabrics, stable isotopes and biomarker analyses. Chem. Geol. 540 (119501) https://doi.org/10.1016/j.chemgeo.2020.119501.

Kneuker, T., Hammer, J., Dohrmann, R., 2020b. PE Experiment: microstructural and mineralogical-geochemical investigations on selected core samples from prospection boreholes BPE-1, BPE-2 and BPE-3. Mont Terri Proj. Techn. Note, 2018–12.

Kneuker, T., Vowinckel, B., Furche, M., Ziefle, G., Maßmann, J., 2021. Opalinus clay from Mont Terri, Switzerland. In: Kolditz, O., Görke, U.-J., Konietzky, H., Maßmann, J., Nest, M., Steeb, H., Wuttke, F., Nagel, T. (Eds.), GeomInt – Mechanical Integrity of Host Rocks. Springer, pp. 16–27.

Kulenkampff, J., Gründig, M., Zakhnini, A., Gerasch, R., Lippmann-Pipke, J., 2015. Process tomography of diffusion, using PET, to evaluate anisotropy and heterogeneity. Clay Miner. 50, 369–375. https://doi.org/10.1180/claymin.2015.050.3.09.

Lange, S., Kowalski, P., Pšenička, M., Klinkenberg, M., Rohmen, S., Bosbach, D., Deissmann, G., 2018. Uptake of ^{226}Ra in cementitious systems: a complementary solution chemistry and atomistic simulation study. Appl. Geochem. 96, 204–216. https://doi.org/10.1016/j.apgeochem.2018.06.015.

Lauber, M., Baeyens, B., Bradbury, M.H., 2000. Physico-chemical characterisation and sorption measurements of Cs, Sr, Ni, Eu, Th, Sn and Se on Opalinus clay from Mont Terri. PSI Rep. 00–10. Paul Scherrer Institut, Villigen, Switzerland.

Lauper, B., Jaeggi, D., Deplazes, G., Foubert, A., 2018. Multi-proxy facies analysis of the Opalinus Clay and depositional implications (Mont Terri rock laboratory,

Switzerland). Swiss J. Geosci. 111, 383–398. https://doi.org/10.1007/s00015-018-0303-x.

Lauper, B., Zimmerli, G.N., Jaeggi, D., Deplazes, G., Wohlwend, S., Rempfer, J., Foubert, 2021. Quantification of lithological heterogeneity within Opalinus Clay: toward a uniform subfacies classification scheme using a novel automated core image recognition tool. Front. Earth Sci. 9 (645596) https://doi.org/10.3389/feart.2021.645596.

Lerouge, C., Maubec, N., Wille, G., Flehoc, C., 2015. GD experiment: geochemical data experiment – analysis of carbonate fraction in Opalinus Clay. Mont Terri Proj. Techn. Note TN-2014-92.

Lüth, S., Steegborn, F., Heberling, F., Beilecke, T., Bosbach, D., Deissmann, G., Geckeis, H., Joseph, C., Liebscher, A., Metz, V., Rebscher, D., Rink, K., Ryberg, T., Schennen, S., 2024. Characterization of heterogeneities in the sandy facies of the Opalinus Clay (Mont Terri underground rock laboratory, Switzerland). Geophys. J. Int. 236, 1342–1359. https://doi.org/10.1093/gji/ggad494.

Maes, N., Moors, H., Dierckx, A., Aertsens, M., Wang, L., de Canniere, P., Put, M., 2001. Studying the migration behaviour of radionuclides in Boom Clay by electromigration. In: Czurda, K., Hötzl, H. (Eds.), Schriftenreihe Angewandte Geologie Karlsruhe, 63, EREM2001, 3rd Symposium and Status Report on Electrokinetic Remediation, pp. 18–20. April 2001, Karlsruhe, Germany.

Marques Fernandes, M., Klinkenberg, M., Baeyens, B., Bosbach, D., Brandt, F., 2023. Adsorption of Ba and ^{226}Ra on illite: a comparative experimental and modelling study. Appl. Geochem. 159, 105815 https://doi.org/10.1016/j.apgeochem.2023.105815Mazurek.

Marques Fernandes, M., Vér, N., Baeyens, B., 2015. Predicting the uptake of Cs, Co, Ni, Eu, Th and U on argillaceous rocks using sorption models for illite. Appl. Geochem. 59, 189–199. https://doi.org/10.1016/j.apgeochem.2015.05.006.

Missana, T., Colàs, E., Grandia, F., Olmeda, J., Mingarro, M., García-Gutiérrez, M., Munier, I., Robinet, J.-C., Grivé, M., 2017. Sorption of radium onto early cretaceous clays (Gault and Plicatules Fm). Implications for a repository of low-level, long-lived radioactive waste. Appl. Geochem. 86, 36–48. https://doi.org/10.1016/j.apgeochem.2017.09.009.

Nagra, 2002. Project Opalinus Clay: safety Report. Demonstration of disposal feasibility for spent fuel, vitrified high-level waste and long-lived intermediate-level waste (Entsorgungsnachweis). Nagra Techn. Rep. NTB 2–5. Nagra, Wettingen, Switzerland.

Nagra, 2022. The site for the deep geological repository – Nagra's proposal. Nagra, Wettingen, Switzerland.

Parkhurst, D.L., Appelo, C.A.J., 2013. Description of input and examples for PHREEQC version 3: a computer program for speciation, batch-reaction, one-dimensional transport, and inverse geochemical calculations. US Geolog. Surv.

Pearson, F.J., 1998. Opalinus clay experimental water: a1 Type, Version 980318. PSI Intern. Rep. TM-44-98-07, Paul Scherrer Inst. Villigen, Switzerland.

Pekala, M., Wersin, P., Rufer, D., Curti, E., 2019. GD experiment: geochemical data experiment – mineralogy of carbonate and sulphate minerals in the Opalinus Clay and adjacent formations. Mont Terri Proj. Technical Report 2018–03.

Philipp, T., Amann-Hildenbrand, A., Laurich, B., Desbois, G., Littke, R., Urai, J.L., 2017. The effect of microstructural heterogeneity on pore size distribution and permeability in Opalinus Clay (Mont Terri, Switzerland): insights from an integrated study of laboratory fluid flow and pore morphology from BIB-SEM images. Geol. Soc. London, Spec. Publ. 454 (1), 85–106. https://doi.org/10.1144/sp454.3.

Poonoosamy, J., Kaspor, A., Rudin, S., Murphy, G.L., Bosbach, D., Deissmann, G., 2023. The use of microfluidic platforms with Raman spectroscopy for investigating the co-precipitation of metals and radionuclides in carbonates. Minerals 13 (636). https://doi.org/10.3390/min13050636.

Rihs, S., Condomines, M., Sigmarsson, O., 2000. U, Ra and Ba incorporation during precipitation of hydrothermal carbonates: implications for ^{226}Ra-Ba dating of impure travertines. Geochem. Cosmochim. Acta 64, 661–671. https://doi.org/10.1016/S0016-7037(99)00344-0.

Saito, A., Kagi, H., Marugata, S., Komatsu, K., Enomoto, D., Maruyama, K., Kawano, J., 2020. Incorporation of Incompatible Strontium and Barium Ions into Calcite (CaCO3) through Amorphous Calcium Carbonate. Minerals 10, 270. https://doi.org/10.3390/min10030270.

Salah, S., Maes, N., Bruggeman, C., Wang, L., Metcalfe, R., Wilson, J., 2017. Compilation of technical notes on less studied elements. Report SCK•CEN ER-0323, SCK CEN. Mol, Belgium.

Scatchard, G., 1936. Concentrated solutions of strong electrolytes. Chem. Rev. 19, 309–327. https://doi.org/10.1021/cr60064a008.

Shannon, R.D., Prewitt, C.T., 1969. Effective ionic radii in oxides and fluorides. Acta Crystallogr. B25, 925–946. https://doi.org/10.1107/S056774086900322.

Shannon, R.D., Prewitt, C.T., 1970. Revised values of effective ionic radii. Acta Crystallogr. B26, 1046–1048. https://doi.org/10.1107/S0567740870003576.

Shao, H., Dmytrieva, S.V., Kolditz, O., Kulik, D.A., Pfingsten, W., Kosakowski, G., 2009. Modeling reactive transport in non-ideal aqueous–solid solution system. Appl. Geochem. 24, 1287–1300. https://doi.org/10.1016/j.apgeochem.2009.04.001.

Singh, B., 1978. Cation exchange. In: Sedimentology, Encyclopedia of Earth Science. Springer, Berlin, Heidelberg, pp. 167–172. https://doi.org/10.1007/3-540-31079-7_38.

SKB, 2011. Long-term Safety for the Final Repository for Spent Nuclear Fuel at Forsmark - Main Report of the SR-Site Project. SKB Technical Report TR-11–01, Svensk Kärnbränslehantering AB, Stockholm, Sweden.

Spahr, D., Bayarjargal, L., Vinograd, V., Luchitskaia, R., Winkler, B., 2023. Incorporation of rare earth elements into $(Ba,Ca)_2(CO_3)_2$. Solid State Sci. 139 (107129) https://doi.org/10.1016/j.solidstatesciences.2023.107129.

Steegborn, F., Heberling, F., Gill, N., Geckeis, H., 2024. Einfluss der Heterogenität von Tongesteinen auf die Rückhaltung von Radionukliden. 4. Tage der Standortauswahl, 18./19.04.2024, Goslar, Germany.

Tachi, Y., Shibutani, T., Sato, H., Yui, M., 2001. Experimental and modeling studies on sorption and diffusion of radium in bentonite. J. Contam. Hydrol. 47, 171–186. https://doi.org/10.1016/S0169-7722(00)00147-9.

Tamamura, S., Takada, T., Tomita, J., Nagao, S., Fukushi, K., Yamamoto, M., 2014. Salinity dependence of ^{226}Ra adsorption on montmorillonite and kaolinite. J. Radioanal. Nucl. Chem. 299, 569–575. https://doi.org/10.1007/s10967-013-2740-3.

Tesoriero, A.J., Pankow, J.F., 1996. Solid solution partitioning of Sr^{2+}, Ba^{2+}, and Cd^{2+} to calcite. Geochem. Cosmochim. Acta 60, 1053–1063. https://doi.org/10.1016/0016-7037(95)00449-1.

Toby, B.H., Von Dreele, R.B., 2013. GSAS-II: the genesis of a modern open-source all purpose crystallography software package. J. Appl. Crystallogr. 46, 544–549. https://doi.org/10.1107/S0021889813003531.

Van Loon, L.R., Baeyens, B., Bradbury, M.H., 2005. Diffusion and retention of sodium and strontium in Opalinus clay: comparison of sorption data from diffusion and batch sorption measurements, and geochemical calculations. Appl. Geochem. 20, 2351–2363. https://doi.org/10.1016/j.apgeochem.2005.08.008.

Vinograd, V.L., Brandt, F., Rozov, K., Klinkenberg, M., Refson, K., Winkler, B., Bosbach, D., 2013. Solid-aqueous equilibrium in the $BaSO_4$-$RaSO_4$-H_2O system: first-principles calculations and a thermodynamic assessment. Geochem. Cosmochim. Acta 122, 398–417. https://doi.org/10.1016/j.gca.2013.08.028.

Vinograd, V.L., Kulik, D.A., Brandt, F., Klinkenberg, M., Weber, J., Winkler, B., Bosbach, D., 2018a. Thermodynamics of the solid solution - aqueous solution system $(Ba,Sr,Ra)SO_4 + H_2O$: I. The effect of strontium content on radium uptake by barite. Appl. Geochem. 89, 59–74. https://doi.org/10.1016/j.apgeochem.2017.11.009.

Vinograd, V.L., Kulik, D.A., Brandt, F., Klinkenberg, M., Weber, J., Winkler, B., Bosbach, D., 2018b. Thermodynamics of the solid solution - aqueous solution system $(Ba,Sr,Ra)SO_4 + H_2O$: II. Radium retention in barite-type minerals at elevated temperatures. Appl. Geochem. 93, 190–208. https://doi.org/10.1016/j.apgeochem.2017.10.019.

Waber, H.N., Rufer, D., 2017. Porewater Geochemistry, Method Comparison and Opalinus Clay – Passwang Formation Interface Study at the Mont Terri URL. Report NWMO-TR-2017-10, Nuclear Waste Management Organization. Canada, Toronto.

Waber, H.N., Schürch, R., 2000. WS-A Experiment: fracture mineralogy and geochemistry as constraints on porewater composition. Mont Terri Proj. Techn. Note TN 99–83, Feder. Off. Topogr. (swisstopo). Wabern, Switzerland.

Wang, J., Guo, X., 2020. Adsorption kinetic models: physical meanings, applications, and solving methods. J. Hazard Mater. 390 (122156) https://doi.org/10.1016/j.jhazmat.2020.122156.

Weber, J., Barthel, J., Klinkenberg, M., Bosbach, D., Kruth, M., Brandt, F., 2017. Retention of ^{226}Ra by barite: the role of internal porosity. Chem. Geol. 466, 722–732. https://doi.org/10.1016/j.chemgeo.2017.07.021.

Wedepohl, K.H., 1971. Environmental influences on the chemical composition of shales and clays. Phys. Chem. Earth 8, 307–333. https://doi.org/10.1016/0079-1946(71)90020-6.

Wersin, P., Mazurek, M., Gimmi, T., 2022. Porewater chemistry of Opalinus clay revisited: findings from 25 years of data collection at the Mont Terri rock laboratory. Appl. Geochem. 138, 105234 https://doi.org/10.1016/j.apgeochem.2022.105234.

Whittaker, M.L., Sun, W., Duggins, D.O., Ceder, G., Joester, D., 2021. Dynamic barriers to crystallization of calcium barium carbonates. Cryst. Growth Des. 21, 4556–4563. https://doi.org/10.1021/acs.cgd.1c00433.

Yoshida, Y., Yoshikawa, H., Nakanishi, T., 2008. Partition coefficients of Ra and Ba in calcite. Geochem. J. 42, 295–304. https://doi.org/10.2343/geochemj.42.295.

Yuan, T., Yang, Y., Ait-Mouheb, N., Deissmann, G., Fischer, C., Stumpf, T., Bosbach, D., 2022. A comparative study on heterogeneity of clay rocks using pore-scale diffusion simulations and experiments. J. Geophys. Res. Solid Earth 127, e2022JB025428. https://doi.org/10.1029/2022JB025428.